2010
2011

GENEESKUNDE

master in de biomedische wetenschappen: klinische moleculaire wetenschappen

Masterproef

Migration of microglia in the embryonic neocortex

Promotor :
Prof. dr. Jean-Michel RIGO

Sophie Smolders

Masterproef voorgedragen tot het bekomen van de graad van master in de biomedische wetenschappen , afstudeerrichting klinische moleculaire wetenschappen

Maastricht University

universiteit hasselt
UNIVERSITEIT VAN DE TOEKOMST

De transnationale Universiteit Limburg is een uniek samenwerkingsverband van twee universiteiten in twee landen: de Universiteit Hasselt en Maastricht University

universiteit hasselt
UNIVERSITEIT VAN DE TOEKOMST

Maastricht University

Universiteit Hasselt | Campus Diepenbeek | Agoralaan Gebouw D | BE-3590 Diepenbeek
Universiteit Hasselt | Campus Hasselt | Martelarenlaan 42 | BE-3500 Hasselt

2010
2011

GENEESKUNDE

master in de biomedische wetenschappen: klinische moleculaire wetenschappen

Masterproef

Migration of microglia in the embryonic neocortex

Promotor :
Prof. dr. Jean-Michel RIGO

Sophie Smolders

Masterproef voorgedragen tot het bekomen van de graad van master in de biomedische wetenschappen , afstudeerrichting klinische moleculaire wetenschappen

Maastricht University

universiteit hasselt
UNIVERSITEIT VAN DE TOEKOMST

TABLE OF CONTENTS

ABBREVIATIONS

BBB	Blood-brain-barrier
BDNF	Brain-derived neurotrophic factor
BSA	Bovine serum albumin
CNS	Central nervous system
CP	Cortical plate
CSF-1R	Colony stimulating factor-1 receptor
CX3CR1	Chemokine (C-X3-C motif) receptor 1 or fractalkine receptor
E	Embryonic day
ECM	Extracellular matrix
eGFP	Enhanced green fluorescent protein
FACS	Fluorescence-activated cell sorting
FNR	Fibronectin receptor
GDNF	Glial-derived neurotrophic factor
GE	Ganglionic eminences
GFAP	Glial fibrillary acidic protein
GLAST	Astrocyte-specific glutamate transporter
i.p.	Intraperitoneally
IFN-γ	Interferon-γ
IZ	Intermediate zone
LMR	Laminin receptor
M-CSF	Macrophage-colony stimulating factor
N-CAM	Neural cell adhesion molecule
NDS	Normal donkey serum
NGF	Nerve growth factor
NGS	Normal goat serum
NT-3	Neurotrophin-3
P	Post-natal day
PBS	Phosphate buffered saline
PFA	Paraformaldehyde
ROS	Reactive oxygen species
rpm	Revolutions per minute
SP	Subplate
TBS	Tris buffered saline
TNF-α	Tumor necrosis factor-α
VZ	Ventricular zone

PREFACE

These past eight months, together with the other internships during my education, were periods of intensive learning, revelations, satisfaction interspersed with some disappointments and stressful combined with fun and relaxed moments. But most of all, this was a period during which I developed confidence, independency and - to some extend I hope – a critical scientific mind. In addition, I found my way to a very enthusiastic and jovial research group, the group of Physiology and Biophysics, which always made me feel right at home. Now my senior internship at the Biomedical Research Institute, Hasselt University has come to its end, I would like to express some words of gratitude towards everybody who helped me along the way.

First of all, I would like to thank Prof. dr. Jean-Michel Rigo for giving me the chance to perform my junior and senior practical training at BIOMED in his research group. Thank you for letting me attend the various lab meetings, for your ever quick responses to all my questions, your proof readings and your support in writing a FWO grant application. Next, I want to thank Nina Swinnen for providing such a good guidance, always staying patient and kind. Thank you Nina for leading me into the world of "the developing microglia" - I surely caught the microbe -, for always being there for me, for giving me allround advice and for your very fast corrections of my thesis. You were a very big support for me during the last two years. I also want to thank Prof. dr. Jerome Hendriks for following my project progress and discussing my results, Prof. dr. Bert Brône for his assistance and suggestions concerning my analyses and the writing of my FWO project and dr. Quirine Swennen for her help and advice concerning the statistical analysis. Many big thanks are addressed to the following persons who played a very important role in the acquisition of my thesis data: Ariel Avila Macaya constructed a set-up and assisted with the time-lapse experiments, Rik Paesen developed and optimized the Angle Tool software in Matlab, Kristof Notelaers postulated many profitable suggestions and assisted with the data analyses. Thank you Nick, Ben, Kristof and Rik for always having your door open and helping me straight away when I popped in countless times for problems or questions about the confocal microscope. Furthermore, I would like to thank my best-friend and student colleague Birgit Baré for her mental support during our whole education and for the enjoyable lunches during the internships. My other fellow students Petra, Winde, Lise, Tijs and Marijke must not be forgotten. Thanks for the interesting discussions and pleasant time we had together in our cozy, little student room.

I am very grateful to my parents for giving me their unconditional support and the opportunity to attend a higher education. Last but not least, thank you Jeroen for never losing your patience with me (which must have been a hell of a job), for always listening to me, for cheering me up when I felt down, and for being happy and proud when things worked out for me.

ABSTRACT

Microglia, also known as the macrophages of the brain, not only serve an immune regulatory purpose, but are also suggested to implement key functions already during development, such as clearing cell debris, influencing neurogenesis, synaptogenesis and neural precursor development. In order to exert these functions, microglia migrate extensively from their entry points to their final locations in the central nervous system. In the developing quail retina, it is known that after invasion, microglia migrate in tangential and radial directions using Müller cells (retinal radial glia) as a substratum. However, the mechanisms for microglial migration during development of the mammalian brain are unknown. Results of our research group show contact between microglia and radial cells during embryogenesis of the mouse neocortex and spinal cord, suggesting that in the mammalian neocortex microglia make contact with radial cells to guide their migration, as cellular scaffolds. Moreover, *in vitro*, microglia express receptors for extracellular matrix (ECM) proteins present on radial cells in the developing brain. In this way, radial cells may also play a role in adhesive guidance. Therefore, the goals of this project were to elucidate the migratory behavior of microglia and the molecular contacts with radial cells during murine embryonic cortical development. Based on immunohistochemical stainings, we observed that microglia mostly resided near the pia and ventricular lining at embryonic day (E) 12.5 and subsequently spread throughout the cortex, together with a significant increase in process length ($p<0.05$) and a clear trend towards increasing branching level. In addition, microglia show equal amounts of radially and tangentially oriented processes from E12.5-E15.5. By means of multi-photon time-lapse microscopy on acute brain slices, we observed that on E14.5 and E15.5 microglia migrate at a similar mean velocity (34.8 µm/h and 32.6 µm/h) in random directions, but according to a general oriented stream. The cellular mechanisms resembled the ones from tangential and radial migration of microglia in the developing quail retina. Their movement pattern was saltatory and during the stationary phases, microglia continuously sent out multiple randomly oriented processes. Immunohistochemical stainings performed on the embryonic mouse neocortex of E12.5-E15.5, showed that the ECM glycoproteins laminin and fibronectin were present on radial cells and that both radial cells and microglial protrusions expressed the corresponding receptors, α6 and α5 integrins (weakly) respectively. Our results suggest that microglia do not migrate according to a collective specific pattern in the developing neocortex, as they do in the retina. However, they show that during migration, microglia can adhere to radial cells through molecular interaction with laminin and fibronectin. Nevertheless, quantification of microglial integrin expression together with the functional assessment of the integrins in a transgene reporter (for both microglia and radial cells) mouse model, will generate conclusive evidence about the cellular and molecular substrates used by migrating microglia in the embryonic neocortex.

SAMENVATTING

Microglia zijn algemeen gekend als de residente macrofagen van de hersenen. Deze cellen hebben niet alleen een immuunregulatoire functie, maar ze worden ook gesuggereerd sleutelrollen te spelen reeds tijdens de embryonale ontwikkeling, zoals onder meer het opruimen van celresten en het beïnvloeden van neurogenese, synaptogenese en neurale precursor ontwikkeling. Hiervoor dienen microglia intensief te migreren vanaf hun invasieplaatsen tot aan hun finale bestemming in het centraal zenuwstelsel. In de ontwikkelende kwartel retina migreren ze in tangentiale en radiale richtingen, gebruikmakend van Müller cellen (radiale glia van de retina). De mechanismen voor microgliale migratie tijdens de hersenontwikkeling van zoogdieren blijven echter onopgehelderd. Resultaten van onze onderzoeksgroep tonen contact aan tussen microglia en radiale cellen tijdens embryogenese van de hersenen en ruggenmerg in de muis, wat suggereert dat microglia radiale cellen gebruiken als een cellulaire leidraad tijdens hun migratie doorheen de neocortex. Daarenboven brengen microglia *in vitro* receptoren voor extracellulaire matrix (ECM) proteïnen tot expressie die aanwezig zijn op radiale cellen tijdens de ontwikkeling. Op basis van deze adhesiereacties kunnen radiale cellen de migratie ook ondersteunen. Dit project beoogde daarom het migratiegedrag van microglia en de moleculaire contacten met radiale cellen tijdens de corticale ontwikkeling van de muis op te helderen. Door middel van immunohistochemie toonden we aan dat microglia zich op dag 12.5 van de embryogenese (E12.5) het dichtst bij de pia en ventriculaire lumen bevonden. Vanaf E13.5 verspreidden ze zich doorheen de cortex met toenemende uitloperlengte ($p<0.05$) en een duidelijke stijgende trend van vertakkingsgraad. Verder vertoonden deze cellen gelijke aantallen tangentiaal en radiaal georiënteerde uitlopers van E12.5 tot E15.5. Door middel van multi-foton time-lapse microscopie op levende hersenslices observeerden we dat microglia op E14.5 en E15.5 aan gelijke snelheden migreerden (34.8 μm/u and 32.6 μm/u), in willekeurige richtingen, maar binnen dezelfde georiënteerde migratiestroom. De cellulaire mechanismen voor migratie waren vergelijkbaar met de mechanismen voor tangentiale en radiale migratie in de ontwikkelende kwartel retina. Hun bewegingspatroon bestaat uit dynamische fasen afgewisseld met stationaire periodes, waarin deze cellen voortdurend verschillende willekeurig georiënteerde uitlopers uitzenden. Immunohistochemie toonde aan dat de ECM glycoproteïnen laminine en fibronectine aanwezig zijn op radiale cellen en dat microgliale uitlopers en radiale cellen de overeenkomende receptoren, α6 and α5 integrine (zwak), tot expressie brengen. Deze resultaten suggereren dat microglia niet collectief migreren volgens een specifiek richtingspatroon, zoals in de retina. Echter kunnen deze cellen wel hechten aan radiale cellen tijdens migratie, door gebruik te maken van de moleculaire interactie met laminine en fibronectine. Kwantificatie van de integrine expressie door microglia samen met de functionele evaluatie van deze integrines in een transgeen reporter (voor zowel microglia als radiale cellen) muismodel, zal afdoend bewijs genereren omtrent de cellulaire en moleculaire substraten gebruikt door migrerende microglia in de embryonale neocortex.

1 INTRODUCTION

A giant leap for neuroscience was made in 1873 when Camillo Golgi developed the silver-chromate staining technique. This discovery allowed neurohistologists to obtain images of neural cells in their entity and morphologically characterize the cells of the nervous system. Franz Nissl was the first to visualize "Stäbchenzellen" (rod cells) of which he suggested to have a capacity for migration and phagocytosis, but it was del Rio Hortega who baptized them "microglia" in 1932. Hortega's cells are generally defined as the macrophages or immune effector cells of the central nervous system (CNS). Primarily, microglia serve to protect or limit the nervous system from damage by setting up an acute neuro-immune response. On the other hand, when detrimental stimuli persist, microglia stay activated and a chronic neuroinflammation arises. Besides their well-discussed immunological functions, microglia are suggested to take part in the development of the CNS. Although their activity in the developing CNS is largely unexplored, it is known that these cells "quietly" phagocytose and remove apoptotic bodies. Furthermore, they are suggested to support the cytoarchitecture and functional maturation of neuronal networks in the CNS. In order to exert this influence, microglia extensively migrate from their points of invasion to their final location.

In contrast to what is known about the migration of neurons, knowledge about the pathways and substrates involved in microglial migration during embryogenesis is scarce. Therefore, this study focuses on the **migratory behavior** of microglia and **molecular contact** with cell partners during murine embryonic cortical development.

1.1 The central nervous system rising

The first major step in CNS development is the formation of three primary embryonic germ layers in the blastocyst. The cells that form the endoderm layer will give rise to structures of the gut and respiratory tract, while the mesodermal cell layer will generate muscle, bone, cartilage and the vascular system. The ectoderm layer will give rise to both epidermal and neuroectodermal stem cells, of which the latter are destined to become the CNS (1). The neuroectoderm subsequently develops into the neural tube containing the neuroepithelial cells, which will give rise to almost all cell types located in the CNS. When the neural tube has closed, the future spinal cord and brain are recognizable (1, 2). The outer layer of the mammalian cerebral hemispheres is called the neocortex. This structure consists of 6 layers and is involved in higher functions such as, language, sense, locomotion, spatial reasoning and consciousness.

1.1.1 Occupants of the neocortex and layer formation

The neuroepithelial cells from the neural tube generate the neural and neuroglial cell types in the neocortex. They all transform into **radial glia**, which act as universal neural precursors (3). Radial glia are bipolar cells that span the entire thickness of the neocortex with their long radial processes extending from the ventricular zone (VZ), where their soma is located, to the pial surface. Furthermore, they show some astrocyte-like properties, such as the expression of the astrocyte-specific glutamate transporter (GLAST) and glial fibrillary acidic protein (GFAP) (4, 5). During early

embryogenesis, radial glia division occurs mainly symmetrical. In this way, the neural precursor population expands quickly in order to enlarge the neocortical area and the progenitor pool. When development progresses, asymmetric cell division becomes predominant. Two different daughter cells are generated, of which one is a radial glia and the other is an intermediate progenitor or a neuron (6). During later stages of development, radial glia transform into astrocytes and oligodendrocytes (3, 6). Suppl. fig. 1 shows a developmental time-line for neurons and macroglia. Neurons are born in the VZ (the deepest zone) and migrate outwards, to a more superficial layer and eventually halt at the Cajal-Retzius cell layer. This first migrating layer of neurons is called the subplate (SP). Migration of these projection neurons results in the inside-out arrangement of the 6 layers (layer VI containing the oldest and layer II/III the youngest neurons) of the adult neocortex (Suppl. fig. 2) (7).

1.1.2 Cell migration modes

Soon after neurons are born, they migrate away from the proliferative regions of the VZ. Two general modes of migration exist in the forebrain. During **tangential** migration, interneurons originating in the ganglionic eminences (GE) migrate parallel to the CNS surface. **Radial** migration is characterized by neurons migrating from the progenitor zone towards the pial surface and by interneurons descending from the cortical plate (CP) towards the VZ in a fashion parallel to the radial glia **(Fig. 1)**. Tangential migration increases the cellular complexity of forebrain circuits by allowing the dispersion of various neuronal cell types originating from regions outside the neocortex and radial migration establishes the general cytoarchitectural framework of the different forebrain subdivisions (1, 8). During tangential migration, distinct types of cell movement

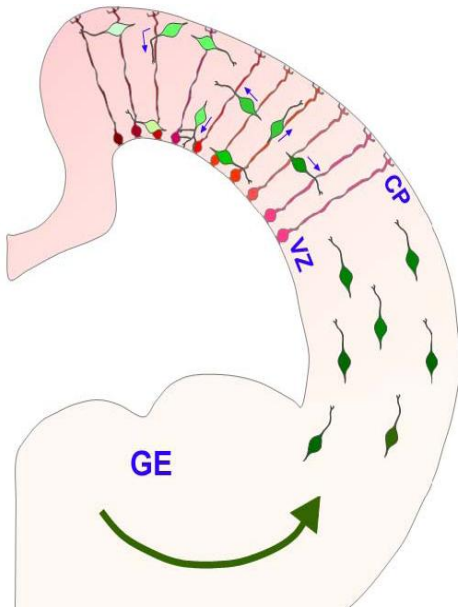

Figure 1. Radial and tangential migration in the embryonic neocortex. Interneurons (green) originating in the GE migrate tangentially to the neocortex and can ascend to the CP or descend in the direction of the VZ along radial gia (red). Neurons born in the VZ migrate radially along radial glia towards the pial surface. GE, Ganglionic eminences; VZ, ventricular zone; CP, Cortical plate. *Adapted from Yokota Y et al. PLoS One 2007, 2(8):e749*

can be distinguished depending primarily on the type of substrate used by migrating cells. Groups of neurons can use each other to promote their migration, follow growing axons to reach their destination or they may not follow specific cellular substrates and instead disperse in a rather individual manner. Radial migration occurs through somal translocation, a cell-independent movement, and by following the process of its progenitor, the radial glial cell, as a guiding-scaffold (8).

1.2 The microglial cell: a versatile outsider

Not all cells dwelling in the CNS find their origin in the neuroepithelium. Until recently, the origin of microglia has been a matter of controversy, but now it is established that they are mesodermally derived immigrant cells (9). They are detectable in the developing brain parenchyma as early as embryonic day (E) 8 in mice, which coincides with the onset of neurogenesis, and fully colonize the CNS by late gestation (9, 10). They account for up to 10% of the total brain cells during the greatest part of development and are present in both white and gray matter. Microglia are generally known as the macrophages or immune effector cells of the CNS. They can adopt two extreme morphological configurations, namely ramified and amoeboid. Ramified microglia are classically defined as 'resting' cells, but this definition is rather misleading since they constantly retract, protrude and move their processes to scan their microenvironment (11). These cells have a slow turn-over rate, a small cellular body and very long, thin branches and they downregulate surface antigen expression (12). The amoeboid morphology, characterized by a large rounded cellular body with a few very thick and short processes, appears primarily during early development and upon encountering activating stimuli, such as cytokines, products of invading organisms, intracellular contents and many others. In response, microglia will upregulate intracellular enzymes, cytokine production and cell surface markers in order to propagate the immune response and/or phagocytose cellular debris. In this state, these cells are also capable of proliferation, migration and antigen presentation (12).

1.2.1 Proposed roles during development

In addition to the well-studied manifold tasks of microglia in acute and chronic neuropathologies, these cells are suggested to implement key functions already during the very early stages of life. Their most evident task comprises clearing enormous amounts of apoptotic neurons, produced in excess during development. Moreover, they can actively regulate cell death via the production of reactive oxygen species (ROS) and various cytokines. Microglia are also able to regulate neuron survival, neurite outgrowth and influence synaptogenesis through the production of thrombospondin, tumor necrosis factor-α (TNF-α) and neurotrophic factors, such as macrophage-colony stimulating factor (M-CSF), nerve growth factor (NGF), brain-derived neurotrophic factor (BDNF), neurotrophin-3 (NT-3) and glial-derived neurotrophic factor (GDNF) (13-16). In addition to regulating synaptogenesis, microglia can eliminate inappropriate synapses labelled by complement through the expression of complement receptors (17, 18). Moreover, it has been proposed that microglia actively monitor and respond to the functional status of synapses (19). Related to the latter, it has even been hypothesized recently that microglia can sense neuronal activity via

receptors and ion-channels and that they modulate the functional integration of neurons (20-22). Furthermore, evidence suggests that microglia are involved in blood vessel formation and recently, they have been found to regulate neural precursor development (23, 24). However, in order to carry out all these tasks, microglia must first travel to the nervous parenchyma, invade the tissue and migrate to their final locations.

1.2.2 Back to the roots

During the last decades, several concepts about the origin of microglia have emerged and consequently a lot of dispute was addressed to this topic. Scientists have proposed these cells to be derived from either neuroectoderm, vascular adventitia, an intrinsic CNS population of hematopoietic stem cells, peripheral mesodermal/mesenchymal tissues or from circulating blood monocytes. Recently, Ginhoux et al. have established that yolk sac macrophages and microglia have the same origin and that **primitive myeloid precursors**, which give rise to adult microglia, arise in the **yolk sac** before E7.5 and travel into the brain through blood vessels between E8.5 and E9.5 **(Fig. 2)**. Moreover, this group proved that these progenitors contribute predominantly to the accomplishment of the adult microglia pool, identifying microglia as an ontogenically distinct population in the mononuclear phagocyte system. Furthermore, they showed that the development of microglia strongly depended on the expression of colony stimulating factor-1 receptor (CSF-1R) (9). In contrast, Chen et al. have recently shown that in the adult mouse brain around 40% of the total microglia population expressed the Homeobox protein Hoxb8 (25). In newborn mice (postnatal day (P)2), they remarked very few Hoxb8-positive microglia in the brain. However, this population increased dramatically between P2 and P14 and was maintained throughout adult life. These results indicate that in the adult brain, at least two pools of microglia are present. One population seems to be of bone marrow origin (derived from circulating monocytes) and colonizes the brain in a later stage of development, corresponding to conclusions of a study by Rezaie et al. in the human fetal brain (26).

1.2.3 The road to colonization

The full colonization of the brain by microglia occurs in three general phases. Upon arrival in the CNS, these cells first **invade** the nervous parenchyma in amoeboid forms probably from microglial "hot spots" in the meninges and ventricular space. These proposed routes of entry are based on the presence of microglia in the ventricular lumen (27) and high microglial density in the pia (27, 28). During later stages of development, when the brain is vascularized but the blood-brain-barrier (BBB) has not formed yet, microglial progenitors may enter the CNS by diapedesis through the blood vessel wall (28, 29). They may use this route to reach their destinations without migrating for long distances. In a second phase, microglia disperse throughout the entire CNS by **proliferation** while **migrating** over long distances through the nervous parenchyma in order to reach their final locations (30-32). The last phase comprises **differentiation** of these amoeboid cells into ramified microglia **(Fig. 2)**(30).

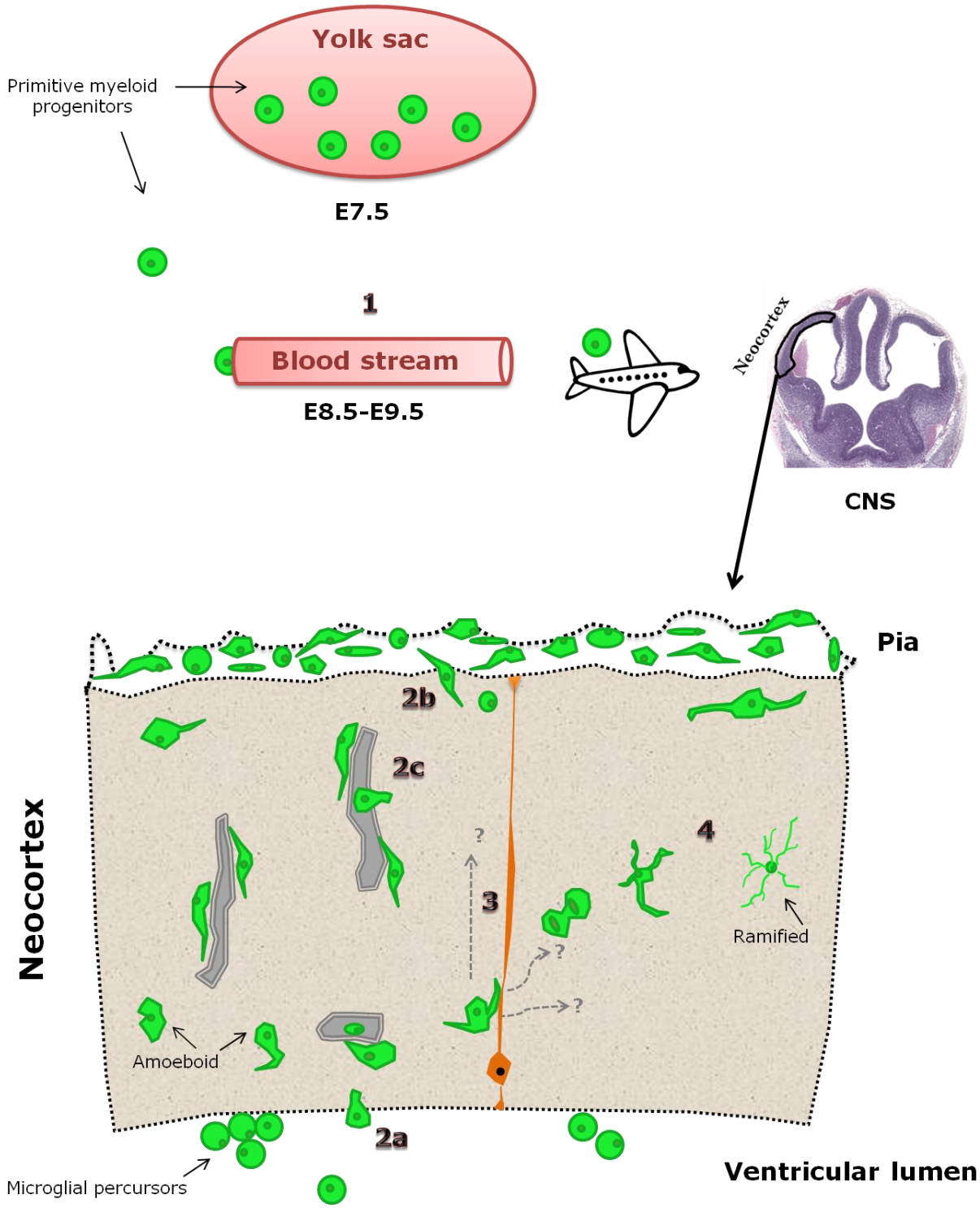

Figure 2. Hypothetical scheme of microglial colonization of the neocortex. 1. Primitive myeloid progenitors arise in the yolk sac around E7.5 and travel to the CNS between E8.5 and E9.5 via the developing circulation. **2.** Once arrived in the CNS, microglial precursors are thought to invade the brain parenchyma in amoeboid forms by crossing the ventricular lining **(2a)**, the pia **(2b)** or in a later phase by penetrating the blood vessel wall (grey filled structures) **(2c)**. **3.** Next, microglia actively proliferate and migrate throughout the tissue to reach their final destinations. Migration can be guided through interaction with radial glia (orange) and/or blood vessels. **4.** In a last phase, these cells differentiate into fully ramified microglia, characterized by multiple thin processes, constantly scanning the microenvironment for changes. Drawings are not to scale. E, embryonic day; CNS, central nervous system.

Studies in the developing quail retina, optic tectum and cerebellum have determined that microglia in regions of laminar organization use definite routes for migration to their final destinations (33-35). Serial sections taken at one-day intervals throughout development of the quail CNS reveal two phases in this process, namely tangential and radial migration. During the first phase, microglia spread in one full single layer throughout each CNS region and this seems to occur along long tangential oriented axonal fascicles, which pass near the microglial entry "hot spots". In the second phase, the cells change direction to reach different depths of the nervous parenchyma (27, 30). The study of Marín-Teva et al. was the first to shed light on the mechanisms involved in long **tangential migration** and migratory behavior of amoeboid microglia *in situ* (36). By means of immunohistochemistry, transmission and scanning electron microscopy the authors established that tangential migration of these cells in the retina takes place on the end-feet of **Müller cells** (retinal radial glia). The cells showed a flattened morphology, probably because of the laminar environment, with extensive lamellipodia. Some microglia were clearly polarized in the movement direction, others were non-polarized with projections radiating in all directions, indicating that these cells explore their substrate and direction determining signals in order to orient their movement. In CNS regions that harbor a non-laminar environment made of axonal fascicles, microglia have a more rounded appearance and show similar morphological characteristics such as a cellular body sending out multiple processes and close contact with the substrate (axons in this case) (30, 36). **Radial migration** towards the pial surface has been described in the retina, optic tectum and cerebellum of the quail embryo. In the retina, microglia were orientated perpendicular to the vitreal surface and they adhered to the processes of Müller cells, indicating these cells as a mechanical substrate for radial migration too (30). Sánchez-López et al. confirmed by means of confocal laser scanning microscopy that radially migrating microglia in the developing quail retina use the processes of s-laminin-expressing Müller cells as a substratum and that these immune cells ramify while radially migrating (37). Moreover, in the developing mouse spinal cord, microglia interact with radial glia through their extending processes (29). In addition, in the developing quail brain stem and murine spinal cord, microglial cells were observed on the wall of blood vessels, interacting with these structures (29, 30). In this way, blood vessels can also function as substrates for migration or microglia could influence vessel formation themselves. Whether the same microglial migration phases and substrates occur in a more complex structure of the mammalian CNS, such as the neocortex, remains an open question. A hypothetical scheme about the colonization of the neocortex by microglia, is presented in **Fig. 2**, based on the previously discussed findings.

In addition to guiding microglia mechanically, Müller cells may also give adhesive support during migration. In the avian developing retina, Müller cells express adhesion molecules, such as laminin and neural cell adhesion molecule (N-CAM) on their end-feet (38). **Laminin** punctuate deposits are also present in a specific spatio-temporal pattern along the course of radial fibers and the pia in the early rat developing brain and mouse developing optic nerve (39, 40). In addition, **fibronectin** is transiently present as punctuate aggregates and closely associates along radial glia in the developing mouse cortex (41, 42). Laminin and fibronectin are both extracellular matrix (ECM) adhesive glycoproteins, which are anchored to fibrous macromolecules, such as collagen, spread in between the cells. Through binding to their specific receptors, called integrins (heterodimeric

transmembrane receptors composed of an α- and a β- subunit), not only cell-cell and cell-matrix adhesion but also cell survival, motility, proliferation, differentiation and gene transcription are regulated (43). Microglia are capable to interact with laminin and fibronectin, since they express the laminin receptor (**α6β1 integrin**, LMR) and the fibronectin receptor (**α5β1 integrin**, FNR) *in vitro*. Furthermore, these cells have shown to adhere to laminin and fibronectin substrates *in vitro* and their activation level together with integrin expression can be regulated by the ECM and cytokines (44, 45).

1.3 Project goals and experimental approach

Despite previous research, the mechanisms for microglial migration in the embryonic neocortex remain unknown and findings in the retina cannot be merely extrapolated to a more complex structure of the CNS such as the neocortex. Preliminary data from our laboratory show that microglia in the murine embryonic neocortex make contact with radial cells. These contacts were also visualized in the embryonic spinal cord (parallel running research) by the research group of P. Legendre (Université Pierre et Marie Curie, Paris, France), collaborating with us (29). Based on previous research and our own preliminary data, we hypothesize that microglia in the embryonic neocortex make use of radial cells to migrate to their final destinations. In this project the transgenic CX3CR1eGFP mouse model will be used, in which enhanced Green Fluorescent Protein (eGFP) expression under the murine fractalkine receptor (CX3CR1) promotor is assigned to monocytes, subsets of NK and dendritic cells, and the CNS microglia (46).

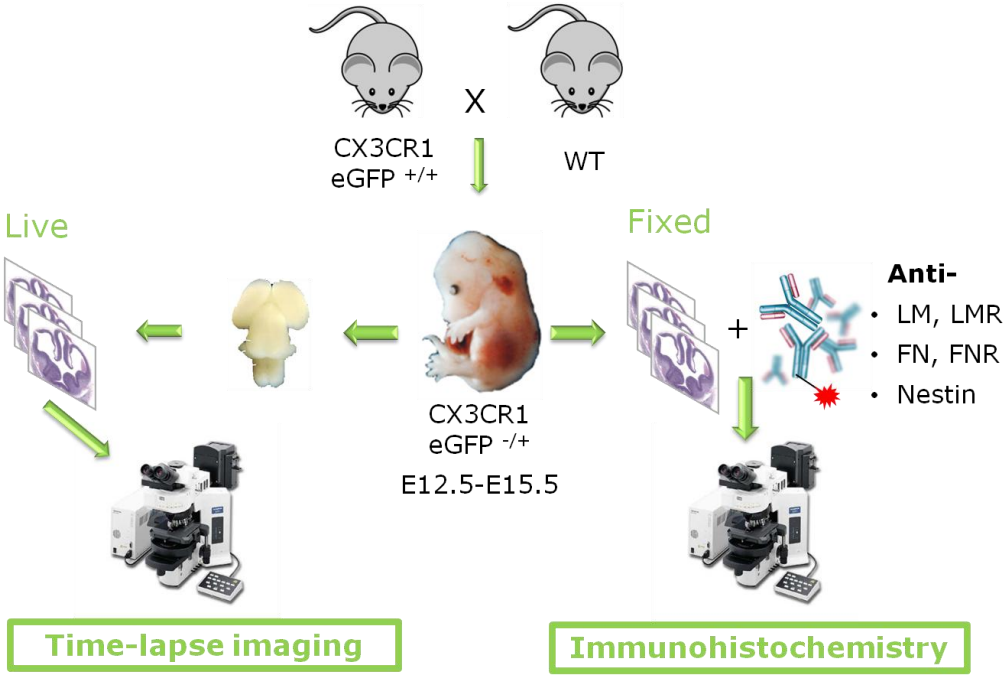

Figure 3. Experimental design. E12.5-E15.5 old heterozygous CX3CR1eGFP mice embryos will be used to conduct immunohistochemical stainings against nestin and adhesion molecules (laminin, fibronectin and their receptors) (right part). In addition, live imaging of microglial migration will be carried out in acute slices of the neocortex (E14.5 and E15.5) (left part). LM, Laminin; LMR, Laminin receptor; FN, Fibronectin; FNR, Fibronectin receptor.

Microglia invade the rodent CNS between E9.5 and E11.5, so in order to consider the migrating population we chose to study the E12.5-E15.5 neocortex (47). To elucidate the migratory behavior of microglia, coronal sections throughout the neocortex from E12.5-E15.5 will be immunostained against nestin (to label radial cells). In this way, an extensive quantification of microglial location, process length and orientation can be performed throughout development. Furthermore, acute embryonic brain slices of E14.5 and E15.5 will be cut and live imaged during 7 hours by means of multi-photon excitation time-lapse microscopy (left part of **Fig. 3**). Between these ages, the increase in neocortical microglial cells is the highest, and is probably due to an increase in migrating cells (own preliminary results). To determine the presence of adhesion molecules on radial cells and microglia, embryonic heads (E12.5-E15.5) will be isolated, fixed and cryosectioned in order to perform immunohistochemistry against laminin, α6 integrin, fibronectin, α5 integrin and nestin (right part of **Fig. 3**).

This project will contribute to the scientific knowledge concerning the development of the central nervous parenchyma. More specifically, our results will provide insight into the microglial colonization process of the neocortex during embryonic development. Furthermore, fundamental insights into cellular mechanisms and adhesion interactions underpinning microglial migratory events will assist in unraveling how maternal inflammation affects microglial influence on CNS development. Maternal immune activation has been associated with an increase in the risk of autism in the offspring. Autism is a neuropsychiatric disorder characterized by impairments in social, behavioral and communicative functions and little is known about its etiology. However, brains of autistic patient were discovered to harbor marked microglial activation (48). The outcome of this project will be combined with recently obtained results from our research group. We showed that microglia in the neocortex of murine embryos from mothers with inflammation acquired a higher activation level than microglia in healthy embryos. Moreover, we determined that microglial density in the maternal inflammation condition is increased in comparison to healthy embryos. This is probably due to an increased invasion and migration of microglial cells into the embryonic CNS. Additionally, it is established that maternal inflammation leads to the upregulation of several pro-inflammatory cytokines, such as TNF-α and interferon-γ (IFN-γ), in the fetal brain and environment (48). These cytokines are proved to raise integrin expression on microglia, which may indicate an increased migratory ability of these cells (45). Our results will determine the most interesting time window to study the effect of maternal inflammation on this process.

2 MATERIALS & METHODS

2.1 Animals and tissue preparation

In order to obtain heterozyguous CX3CR1 eGFP$^{+/-}$ embryos, C57BL/6 Wild type (obtained from Harlan, the Netherlands) and C57BL/6 CX3CR1 eGFP$^{+/+}$ mice (obtained from EMMA with approval of Stephen Jung (46)) were mated overnight. The next morning, female mice were checked for the presence of a copulation plug. When present, this day was considered as E0.5. Starting from E6.5, mice were observed and scored every two days for weight, lethargy, ptosis, pilo-erection, dried tear fluid, breathing and food and water intake. On E11.5, dams were intraperitoneally (i.p.) injected with 100µl sterile phosphate-buffered saline (PBS) (pH 7.4) in order to compare these healthy embryos to those subjected to maternal inflammation in a parallel running study. All experiments were conducted with the approval of the Ethical Committee on Animal Research of Hasselt University. Mice were maintained in the animal facility of Hasselt University in accordance with the guidelines of the Belgian Law and the European Council Directive.

Pregnant mice were sacrificed by means of cervical dislocation at E12.5–E15.5. The uterus and embryos were isolated and kept in PBS-glucose (pH 7.4; 25mM) at 4°C. Subsequently, embryos were decapitated and heads were immediately fixed by immersion in 4% paraformaldehyde (PFA) for 3 hours at 4°C. After fixation, heads were washed in PBS and cryoprotected in PBS-30% sucrose at 4°C. When the embryonic heads were saturated, they were imbedded in Optimal Cutting Temperature (O.C.T.) compound (Tissue-Tek, Sakura Finetek Belgium, Berchem), frozen in liquid nitrogen and stored at -80°C until sectioning. 10µm-thick coronal sections were cut in the GE region on a Leica CM3050S cryostat, mounted onto Superfrost Plus glasses (Menzel-Gläser, Thermo Scientific, Braunschweig) and stored at -20°C. All steps occurred as much as possible in the dark.

2.2 Immunohistochemical stainings

All primary and secondary antibodies and dilutions used are listed in **Table 1 and 2**. Prior to use, all secondary antibodies were centrifuged 5min at 5000 revolutions per minute (rpm). All steps occurred as much as possible in the dark in order to prevent bleaching of the eGFP fluorescent microglia and the labelled secondary antibodies. After labelling, sections were conserved at 4°C. Negative staining controls for the secondary antibodies were performed by omitting the primary antibodies. Positive staining controls for the adhesion molecules are listed in **Table 1**.

2.2.1 Laminin, fibronectin, alpha6 and alpha5 integrin

Coronal brain sections were thawed at room temperature and washed 3X5min in PBS. All following steps occurred at room temperature, unless stated otherwise. After washing, sections were blocked by 1h incubation with PBS-20%NXS (Normal Goat or Donkey Serum, Chemicon, Brussels). Next, sections were incubated overnight at 4°C with the primary antibody diluted in PBS-1%NXS. The next day, sections were washed 3x10min in PBS. Sections were incubated 60min with the secondary antibody, labelled with Alexa 555 and diluted in PBS-1%NXS. After incubation, sections were washed 3x5min in PBS and submerged in distilled water. Corners were dried and vectashield

(DAPI incl.) (Vector, Burlingame) was dropped on the section. A cover slip was put on top and after drying, sealed with nail polish. Immunolabeled sections were conserved at 4°C. Staining controls for the secondary antibodies were performed by omitting the primary antibodies.

2.2.2 Nestin

Coronal brain sections were thawed and washed 2X5min in Tris-Buffered Saline (TBS)-0.025% Triton-X100 (Sigma Aldrich, Bornem). All the following steps occurred at room temperature. After washing, sections were permeabilized and blocked by 2h incubation with TBS-1% bovine serum albumin (BSA) with 10%NGS and 0.5%TritonX100. Next, sections were incubated 2h with the primary nestin antibody diluted in TBS-1%BSA. Afterwards, sections were washed 2x5 min in TBS-0.025% Triton-X100 and incubated 1h with the secondary antibody labelled with Alexa555 diluted in TBS-1%BSA. After incubation, sections were washed 3x5min in TBS and submerged in distilled water. Corners were dried and vectashield (DAPI incl.) was dropped on the section. A cover slip was put on top and after drying, sealed with nail polish.

2.2.3 Doublestainings

Doublestainings were performed sequentially. Sections were first stained for the adhesion molecules (laminin, fibronectin, α6 or α5 integrin), next the submersion step in distilled water was omitted and the staining protocol for nestin was adopted. Adhesion molecules were labelled with a secondary antibody conjugated with Alexa555, nestin was labelled with a secondary antibody conjugated with Alexa647.

Table 1. Primary antibodies for immunohistochemical staining

Markers	Host/Isotype	Company & reference	Dilution	Pos. control
Laminin	Polyclonal rabbit anti-mouse	Abcam, Ab11575	1:200	Skeletal muscle
Fibronectin	Polyclonal rabbit anti-mouse	Abcam, Ab2413	1:100	Kidney
α6 integrin	Monoclonal rat anti-mouse, IgG2a	Abcam, Ab19765, clone Go H3	1:500	Epithelium
α5 integrin	Monoclonal rat anti-mouse, IgG2a	Acris, SM2100PS, clone MFR5 (5H10)	1:500	Embryonic body
Nestin	Monoclonal rat anti-mouse, IgG2b	Abcam, Ab81462, clone 7A3	1:500	

Table 2. Secondary antibodies for immunohistochemical staining

Secondary antibody	Company & reference	Dilution
Donkey-anti-rabbit-A555	Invitrogen, A31572	1:500
Goat-anti-rat-A555	Invitrogen, A21434	1:500
Goat-anti-rat-A647	Invitrogen, A21247	1:500

2.3 Microscopy of fixed tissue

2.3.1 Wide field fluorescence microscopy

Images of sections were acquired using a Digital sight DS-2MBWc fluorescence camera adapted on a Nikon Eclipse 80i microscope. Nikon NIS-Elements BR 3.10 software was used. Blanks were photographed first and camera settings (exposure and gain) were set in order that no signal for the TRITC-channel could be detected. Overlay pictures of DAPI, FITC and TRITC channels were obtained using these blank settings, to manually subtract the background signal. For the quantification of microglial location, process length and orientation in the neocortex, nestin (A555) stainings were photographed with a Nikon Plan Fluor 20x/0.5 objective. The stainings for adhesion molecules (labelled with A555) were photographed with a Nikon Plan 10x/0.25 objective and a 20x objective. A 40x Nikon Plan Fluor/0.75 objective was used to capture cells of interest. Images were converted to RGB by means of the Nis-Elements Viewer software. Images were further color balanced and analyzed using ImageJ 1.44 (NIH, USA; http//rsb.info.nih.gov/ij/).

2.3.2 Confocal microscopy

Doublestained sections were analyzed using an inverted Zeiss Axiovert 200M microscope attached to a Zeiss LSM 510 Meta confocal laser scanning system. Plane images and Z-stacks (serial optical sections) with an interval of 0.50-1µm were acquired using a 40x LD C-Apochomat/1.1 W Korr UV-Vis-IR objective (NA=1.1). A 4x digital zoom was applied to cells of interest. An Arg-ion laser at 488nm, a HeNe laser at 543 and 633 nm and a Mai Tai DeepSee Ti:Saphire laser (Spectra-Physics) tuned at 710nm were used for excitation of eGFP, Alexa555, Alexa647 and DAPI, respectively. Image acquisition (512x512;12-bit) took place with the Zeiss Laser scanning microscope LSM510 software (version 4.2 SP1). Images were colour balanced and prepared using Zeiss LSM Image Browser and ImageJ.

2.4 Quantification of microglial location, process length and orientation

Quantification was performed on nestin stainings (images of 20x magnification), in order to determine the exact angle between a microglial process and the contacting radial fiber. Images for quantification were converted to RGB by means of the Nis-Elements Viewer software. In ImageJ, the blue colour (DAPI) was removed and the green (microglia) and red (radial cells) channels were colour balanced in order to perfectly visualize the microglial cell and its protrusions, as well as the

radial cells. Pictures (1600x1200; RGB) were loaded as projects in the home-made Matlab Plug-in "Angle" (developed by Rik Paesen, Group of Biophysics, Biomedical Research Institute, Diepenbeek). Using this program, the parameters listed in **Table 3** were measured for each microglial cell located in the neocortex and listed in Excel 2007. To determine the process angle, first a reference was drawn over the contacting radial fiber. Second, a line was drawn over the process, starting on the edge of the soma and ending at the end of the process. The program subsequently calculated the angle of the "process line" in reference to the "radial fiber line (=0°)". An example of the line drawing in "Angle" is given in **Fig. 4**. In addition, to each microglial process a category number of certainty (1-3) was allocated. Processes which were very faint or far separated from the microglial soma were categorized as 1. Category 2 was comprised of processes which were faint or very close separated from the soma. Processes which were sharp and connected to the soma were categorized as 3. Processes categorized as 1 were excluded from the Excel database and the statistical analysis. After data collection, microglial location was calculated as a percentage of the cortical thickness (0% correlating to the ventricular lining; 100% correlating to the pia) and processes were considered to be tangentially oriented if their angles (absolute values) were situated between 45° and 135° or radially oriented if their angles were smaller than 45° or larger than 135°.

Table 3. Parameters for quantification

Parameter	Definition	Unit
Microglial location	Straight length between the ventricular lining and the middle of the microglial cell soma	µm
Thickness of the neocortex	Straight length between the ventricular lining and the pia, running through the microglial soma in question	µm
Process length	Length between the edge of the soma and the end of the process, measured with the polygon tool	µm
Process orientation	Angle between the process and the contacting radial fiber as a reference ranging from -180° till +180°)	Degrees
Zone*	Zone of the neocortex in which the cell is located Ventricular zone (VZ), Intermediate zone (IZ) or cortical plate (CP)	VZ/IZ/CP

* Zones were defined based on clear morphological borders in the anatomical organization of the neocortex using DAPI staining. The classification of the zones is depicted in Suppl. fig. 3.

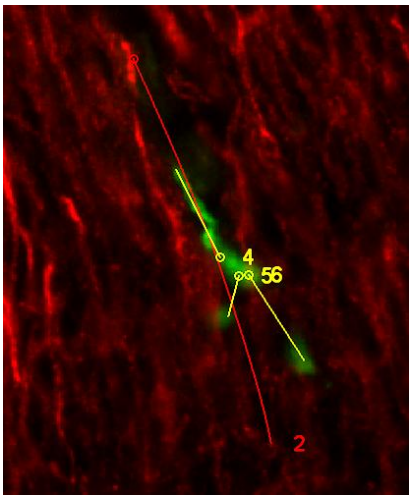

Figure 4. Microglial cell and radial fibers for quantitative analysis in Angle-Matlab. Red, Radial fibers; Green, microglia. Red line, reference drawn over radial fiber; Yellow lines: process lines to determine the angle with the reference.

2.5 Time-lapse imaging

2.5.1 Acute ex vivo slice preparation

Pregnant (E14.5 and E15.5) mice (carrying CX3CR1 eGFP$^{+/-}$ embryos) were sacrificed by means of cervical dislocation. The uterus and embryos were isolated and kept in PBS-glucose at 4°C. Next, embryos were decapitated using small dissection scissors and placed under a microscope on a cold plate for dissection of the brain. The head was placed with the rostral part pointing up and the skin on top was peeled away using forceps in order to let the telencephalon and mesencephalon pop out. The rest of the tissue was pulled apart until the olfactory bulb with the telencephalon, mesencephalon and rhombencephalon with brain stem remained **(Fig. 5)**. Next, dissected brains were immobilized in 3% low melting agarose (Fisher Scientific, New Jersey) in PBS and put on ice during 60min in order to complete the agarose polymerization. Subsequently, agarose cubes containing the embryonic brains were coronally sectioned (300µm) with a Microm HM650V Vibrating Blade Microtome, in a bath of PBS-glucose at 4°C. A 6-well plate was prepared with 1ml Neurobasal medium containing 2mM L-glutamine, 2% B27 supplement, 1% N2 supplement and 0.5% penicillin-streptomycin (all from Invitrogen). MilliCell organotypic inserts (Millipore, MA, USA) were then placed in the wells and 1ml medium was added on top of the inserts. Acute slices were mounted on these inserts and in order to keep them in semi-hydrous conditions, the medium on top was discarded and the sections were maintained at 37°C, 5% CO_2 during 1h for equilibration.

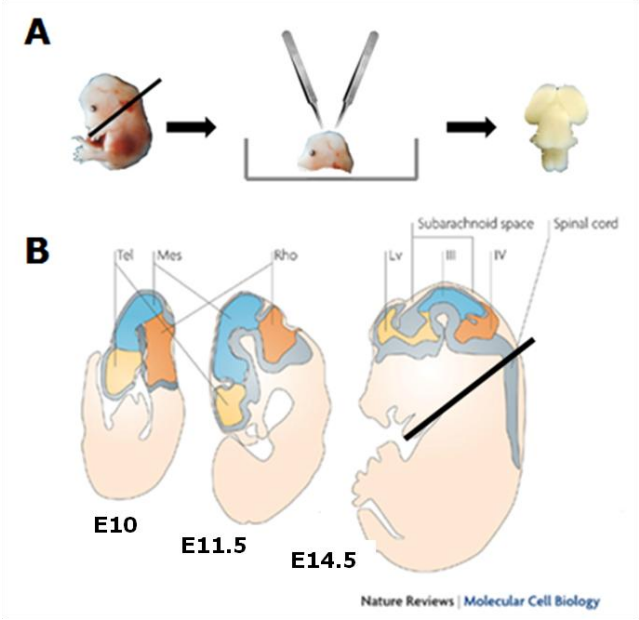

Figure 5. Brain dissection procedure. A. Embryo is decapitated, the head is transferred to a petri dish and skin on top of the head is peeled off using forceps. **B.** Other tissues are removed until the telencephalon (Tel; yellow), mesencephalon (Mes; Blue) and rhombencephalon (Rho; Orange) with brain stem remain. *B. Adapted from Fliegauf M, Benzing T, Omran H. Nat Rev Mol Cell Biol 2007, 8(11):880-93*

2.5.2 Multi-photon excitation time-lapse microscopy

After equilibration, a slice was transferred on its insert to a glass bottom microwell dish (MatTek Corporation, Ashland, MA, USA) and medium for time-lapse imaging with an inverted Zeiss Axiovert 200M microscope attached to a Zeiss LSM 510 Meta confocal laser scanning system. The previous mentioned LSM510 software was used. A Mai Tai DeepSee Ti:Saphire laser (Spectra-Physics) tuned at 900nm was used to excite eGFP expressing microglia. Prior to recording, the slice was rotated in such a way that the pia was located at the top of the imaging field and parallel to the X-axis, so the X coordinate can be equated with the tangential direction and the Y coordinate with radial direction. Z-stacks of the neocortex were repeatedly acquired using a 20x EC plan-Neofluar/0.5 (NA=0.5) objective, every 10min for 7h. Z-stacks were 72µm in height with serial optical sections (1024X1024; 8-bit) every 8µm (in total 10 optical sections per Z-stack). In order to image the non-activated microglial cell population, recordings occurred at a minimum depth of 50µm under the cutting surface of the slice. Measurements occurred at semi-hydrous conditions, 37°C and 5% CO_2 in an insulated chamber. The measurements at E14.5 took place in a Styrofoam insulated Incubator-S (PeCon), with direct supply of 37°C humified air with 5% CO_2 (air supply system constructed by Ariel Avila Macaya). A Heating Insert P and Objective Heater were used to ensure a stable temperature, which was regulated by a Tempcontrol 37-2 digital 2-channel (all from PeCon). For the measurement on E15.5, a Zeiss live cell imaging chamber (Incubator XL-3 LSM DARK) was adapted on the microscope. The chamber was heated by constant air provision at 37°C. Heating Insert P, CO_2-Cover PM and Humidifier Module 1, were used to supply humified air with 5%CO_2 to the tissue (all from PeCon). Temperature and CO_2 were regulated by a heating unit, a Tempcontrol 37-2 digital 2-channel and a CO_2-Controller (all from PeCon). In order to design a

time-lapse movie, a Z-projection was made from the hyperstack and compiled into a windows media player movie (AVI format) using ImageJ.

2.5.3 Migration track analysis

Time-lapse Z-stacks were concatenated, converted into hyperstacks and color balanced using ImageJ. An ImageJ plug-in "MTrackJ" was used to manually track migration paths of microglia. To this end, the cell soma was identified on each time point in the optical section which showed the brightest eGFP signal. X,Y and Z calibrated coordinates (µm) were automatically registered upon every identification. For each cell and time point the software calculated migrated length (µm) and velocity (µm/min). Only cells present in the field of view for the entire 7 hours were included in the analysis. Data were exported to Excel 2007 and the mean migration velocity per cell was calculated. In addition, absolute values of migrated length between successive time points was computed for X,Y and Z coordinates. Cells were defined to migrate mainly radial when the sum of the former mentioned absolute values for Y was larger than the sum for X. Conversely, the main migration direction was considered tangential when the sum of the absolute values for X was larger than the sum for Y. A three dimensional view of the covered migration pathways was established by plotting the cell's coordinates (X,Y,Z in µm) for each time point into 3-D graphs in OriginPro 8 SR0 v8.0724 (OriginLab Corporation, Northampton, MA, USA).

2.6 Statistical analysis

Statistical analysis was performed using GraphPad Prism (version 5.01) for Windows (GraphPad Software, San Diego California USA, www.graphpad.com). Either raw data or mean ± SEM values are shown with "n" being the amount of cells or processes, or "N" being the amount of independent embryos. Depending on the data, the appropriate parametric (One-way ANOVA followed by Bonferroni's Multiple Comparison test, Two-way ANOVA) or nonparametric (Mann Whitney test, Kruskal-Wallis test followed by Dunn's Multiple Comparison test) was applied. Differences with a p-value<0.05 were considered significant. The level of significance is indicated as follows: ~ =p<0.1; * =p<0.05; ** =p<0.01 and *** =p<0.001.

3 RESULTS AND DISCUSSION

In this study, it was hypothesized that microglia in the mouse embryonic neocortex make use of radial cells to migrate to their final destinations. In order to evaluate our hypothesis, we aimed to elucidate the migratory behavior of microglia during development and to determine the presence of adhesion molecules on microglia and radial cells, which would allow them to interact with each other. To this end, first, a more elaborate morphological profile of microglia in the E12.5-E15.5 neocortex was established, based on immunohistochemical stainings against nestin. Second, the migration of microglia was recorded *ex vivo* during 7 hours in acute E14.5 and E15.5 brain slices. Third, the presence of the ECM molecules laminin and fibronectin, together with the expression of the corresponding receptors α6 and α5 integrin was assessed in the E12.5-E15.5 neocortex by means of immunohistochemistry. Heterozygous transgenic CX3CR1eGFP mice embryos were used in all experiments, in order to instantly visualize microglia.

3.1 Microglial location, branching level and process orientation

To elucidate the migratory behavior of microglia, a morphological profile of microglia during embryonic development was established. Fixed brain sections of E12.5-E15.5 old embryos were immunostained for nestin, a marker for the neural precursor cells of the subventricular zone, namely the radial cells (29). Microglial location in the neocortex, the amount and length of protrusions together with their orientation (degrees in reference to the radial fibers) were manually assessed in a home-made matlab plugin, "Angle", as described in section 2.4.

When evaluating microglial location, the neocortical area was split up into two parts for statistical purposes, namely the ventricular half (the part of the parenchyma joined to the ventricular lumen) and the cortical half (the part joined to the pia). At E12.5, microglia are situated in close vicinity of the ventricular lining **(Fig. 6-A)** and pia **(Fig. 6-B)**. Starting from E13.5, these cells were distributed more evenly in neocortex, so also in the intermediate layers. However, they did not colonize each cortical layer uniformly, since at E14.5 a trend can be visualized towards less microglia being located in the CP ($p<0.1$), which turns significant at E15.5 ($p<0.05$) (Suppl. fig. 4 and 5). **Fig. 6** shows that in the ventricular half, microglial location increases significantly (19.48 ± 2.31% at E12.5 versus 31.49 ± 2.77% and 31.33 ± 1.64% at E13.5 and E14.5 respectively, $p<0.01$), while in the cortical half microglial location decreases significantly (89.16 ± 1.37% at E12.5 versus 75.15 ± 1.53% and 67.24 ± 1.70% at E14.5 and E15.5, respectively, $p<0.001$) with increasing age. The E12.5 microglial distribution pattern suggests that these cells start to migrate from the proposed sites of entry (ventricular lining and pia (27)) in a radial fashion, in order to populate the intermediate cortical layers. In the context of invasion points, we observed amoeboid microglia in the ventricular lumen sending out very short processes contacting the ventricular lining, penetrating it and continuing their migratory journey (see Suppl. fig. 6). Furthermore, microglial/monocytic precursors characterized by an amoeboid morphology and a low eGFP expression (faint in comparison to the resident microglia) were remarked inside blood vessels **(Fig. 17-D1 and 20-C3)**. These observations concur with findings in other studies in the mammalian and avian CNS (27, 29, 30, 49).

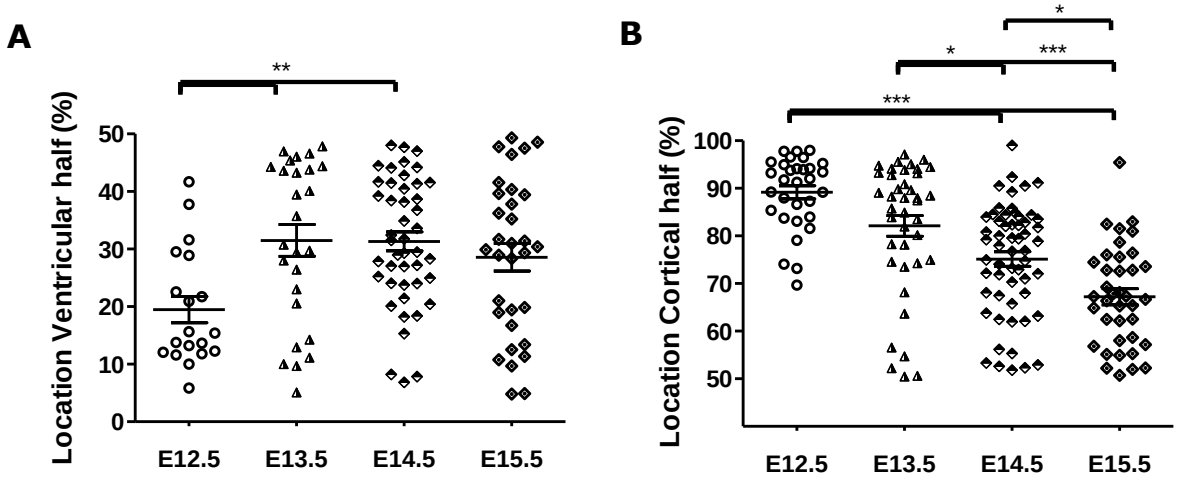

Figure 6. Microglial location in the embryonic neocortex. A. Location of microglia in the ventricular half of the neocortex. **B.** Location of microglia in the cortical half of the neocortex. Microglial location is expressed in percentage of the entire thickness of the neocortex, with 0% corresponding to the ventricular lining and 100% to the pia. At E12.5, microglia are mostly located close to the ventricular lining **(A)** and to the pia **(B)**. From E13.5, these cells start to spread in order to populate the entire neocortex at older ages. Means ± SEM are indicated. N=3 for all ages. In A, n=19;26;45;32 and in B, n=31;40;57;38 for E12.5;13.5;14.5;15.5. One-way Anova followed by Bonferroni's Multiple Comparison test (A) and Kruskal-Wallis analysis followed by Dunn's Multiple Comparison test (B) were applied. *=p<0.05; **=p<0.01; ***=p<0.001.

When development proceeds, microglial processes become progressively longer **(Fig. 7-A)**. Protrusions on E15.5 measured 11.35 ± 0,67 μm and are significantly longer than the microglial processes on E12.5 being 8.58 ± 0.57 μm on average ($p<0.05$). Furthermore, microglia tend to increase their ramification level from E12.5 (1.10 ± 0.16 processes per cell) until E13.5 (1.84 ± 0.13 processes per cell) ($p<0.1$) **(Fig. 7-B)**. When cells were categorized into two morphological classes, namely amoeboid and bearing one or more processes, a decreasing trend was present in the amoeboid microglial population along development. Furthermore, the percentage of microglia bearing one or more processes exhibited an increasing trend from E12.5-E15.5 **(Fig. 7-C)**.

Despite the fact that the differences in ramification degree were not significant, the microglial branching level evaluated in this study is very likely an underestimation of the true amount of processes per cell. Our quantifications are based on 10μm thick organotypic sections, which allows us to gather relatively fast *in situ* information in one plane. However, since microglial protrusions can achieve long lengths (up to 40μm at E15.5, own observations) in three dimensions, it is highly probable that some protrusions were missed because of the sectioning. Especially at E15.5, various thin, individual protrusions were observed in the neocortex in the absence of a corresponding cell soma. Microglia are generally known to enter the nervous parenchyma in amoeboid forms and to differentiate further into ramified cells as the embryo ages (49). The amoeboid morphology is usually seen as a stage of activation – during which the cell is capable of phagocytosis and migration - in contrast with the "resting" or more appropriate "scanning" ramified microglia. Consequently, the rate of movement of ramified microglia has been reported to increase as the number of cell branches decreases (50). In this way, the progressive rise in microglial protrusions throughout development could be considered as a hallmark of differentiation towards the scanning phenotype, associated with a decline in migratory capacity.

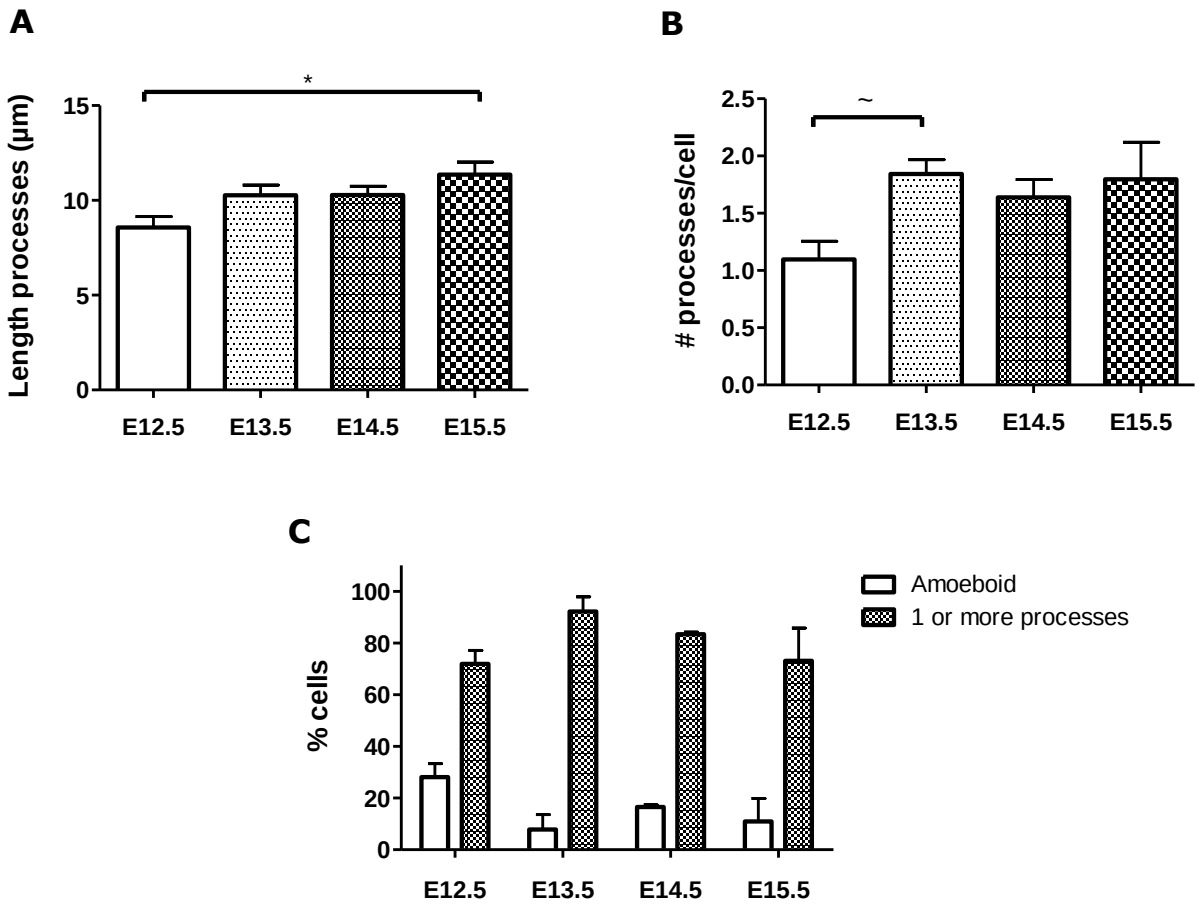

Figure 7. Microglial branching level and process length in the embryonic neocortex. A. Length (µm) of microglial protrusions from E12.5 until E15.5. During development, the length of microglial processes increases significantly (n=55;122;165;128 for E12.5;13.5;14.5;15.5). **B.** General microglial branching level. The amount of processes per microglial cell tends to increase when the embryo ages (N=3 for all ages). **C.** Percentage of amoeboid microglia and cells with processes. The percentage of amoeboid microglia tends to decrease while the percentage of microglia with 1 or more processes tends to increase throughout development (N=3 for all categories and ages). All points represent the mean ± SEM. Mann Whitney test was applied for A,B and Two-way ANOVA for C. ~=p<0.1; *=p<0.05.

As a last parameter, the angle formed between the microglial process and the radial fiber contacting it, was calculated. Processes were considered radially oriented if their angle was to some extent parallel to the radial fibers (0°-45° or 135°-180°) and tangentially oriented, if the angle was transverse to this direction (45°-135°). **Fig. 8-A** shows that there was no significant difference between the percentage of tangentially versus radially oriented protrusions from E12.5-E15.5. However, a slight trend can be noticed at E12.5-E13.5, which is opposite to the trend at E14.5-E15.5. At the earlier ages, microglial process inclined to be more tangentially oriented, while at the later ages, they tended to be more radially oriented. These findings could imply that microglia at E12.5-E13.5 migrate more tangentially and that at E14.5-E15.5, they migrate more radially. In order to seek for location-dependent orientations, data were subsequently divided into two groups (processes located in the ventricular half or in the cortical half), but no significant difference concerning the distribution of tangential and radial processes was obtained (data not shown).

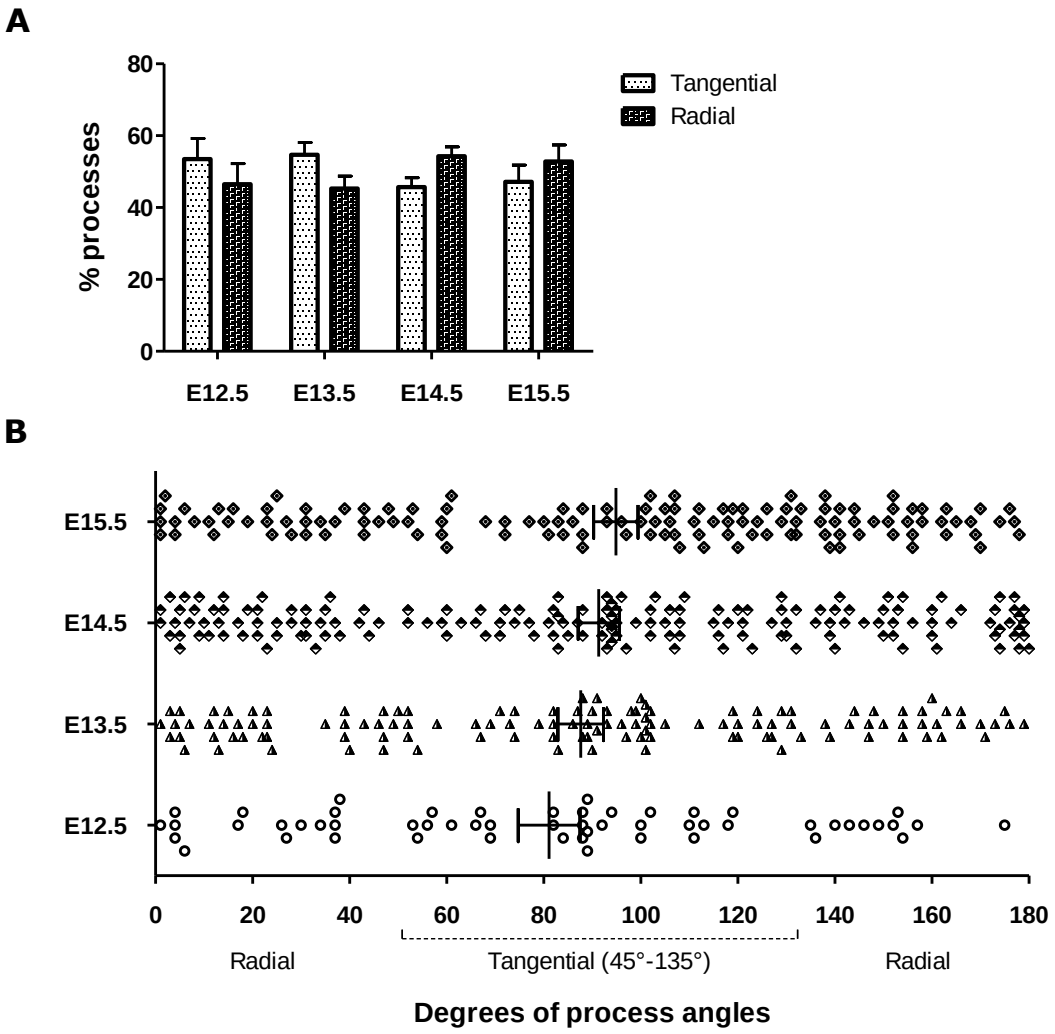

Figure 8. Orientation of microglial processes in the embryonic neocortex. Process orientation was considered tangential if the angle between itself and the contacting radial glial fiber was situated between 45° and 135°, and radial if it was not. **A.** Percentage of microglial processes oriented tangentially and radially. The percentage tangentially and radially oriented processes stays equal from E12.5 until E15.5 (N=3 for all ages). **B.** Exact orientation of microglial processes from E12.5 until E15.5. Note that the angles are distributed uniformly (n=55;122;165;128 for E12.5;13.5;14.5;15.5). Means ± SEM are indicated. Mann Whitney test (A) and Kruskal-Wallis test followed by Dunn's Multiple Comparison test (B) were applied.

When the raw data (angles in degrees) were plotted **(Fig. 8-B)**, a uniform distribution of the angles can be noted at each age. These results may imply that microglia do not migrate in one specific direction, or that these cells may constantly move their processes and change orientation in such a way that this parameter is not a strong predictor of the eventual migration direction of the cell. Moreover, the edge under which the tissue was cryosectioned influenced the view of radial fibers along their full course. In this way, the radial fibers sometimes showed a discontinuous path. Although this was not often the case, it implies that the fixed analysis cannot be considered as fully accurate and that in the future, this analysis will only be based on sections in which the radial fibers show a continuous course.

All together, the results of the fixed analysis suggest that microglia start to colonize the neocortex from the ventricular lining and pia. During this process, they can migrate in different directions, but possibly still in a main radial stream in order to reach the intermediate cortical layers. Moreover, the increase in protrusion length and trend towards an increasing branching level with rising embryonic age, may indicate the start of differentiation towards ramified, scanning cells. To better define the migratory behavior and dynamics of microglia *in situ*, we subsequently recorded migration in acute brain slices.

3.2 *Ex vivo* migration of microglia in the E14.5-E15.5 neocortex

In order to further elucidate the migratory behavior of microglia, microglial migration was recorded *ex vivo*. To this end, 300µm-thick acute coronal brain slices were cut from E14.5 and E15.5 embryos and imaged by means of multi-photon excitation microscopy. Slices were imaged starting from a minimum depth of 50µm under the cutting surface of the slice, in order to image the non-activated microglial cell population. During the experiment, the tissue was kept at 37°C and 5% CO_2 in semi-hydrous conditions. Z-stacks were recorded every 10 minutes during 7 hours and microglial migration tracks were analyzed using MTrackJ in ImageJ. The pia was always located on top, parallel to the X-axis.

The time-lapse movies showed that all cells constantly sent out and retracted processes. Microglia migrating towards each other and sending out thin protrusions to make contact for a period and retracting their process afterwards, were regularly remarked **(Fig. 9)**. These multiple contacts imply that the embryonic microglial network is highly communicative and that these cells could exchange signals to direct their movement, after the contact has taken place. Furthermore, cells situated in the pia were found to exit this structure and enter the cortical parenchyma. Conversely, microglia located in the parenchyma were seen to migrate into the pia. Unfortunately, a clear demarcation between the ventricular lumen and parenchyma was absent, so microglia entering the neocortex from the ventricular lumen could not be distinguished. Mitotic cells were not seen in the time span of 7 hours.

A

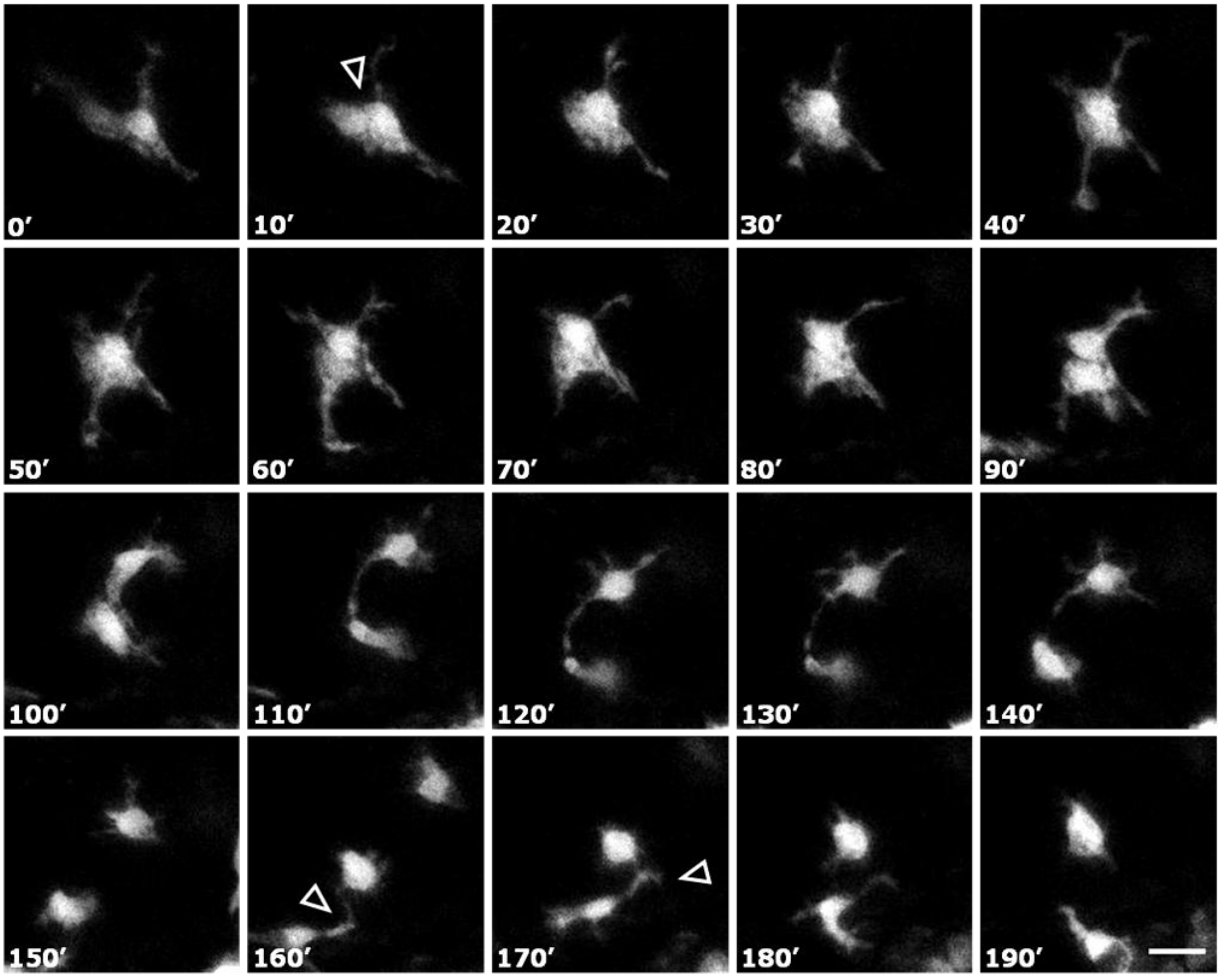

B

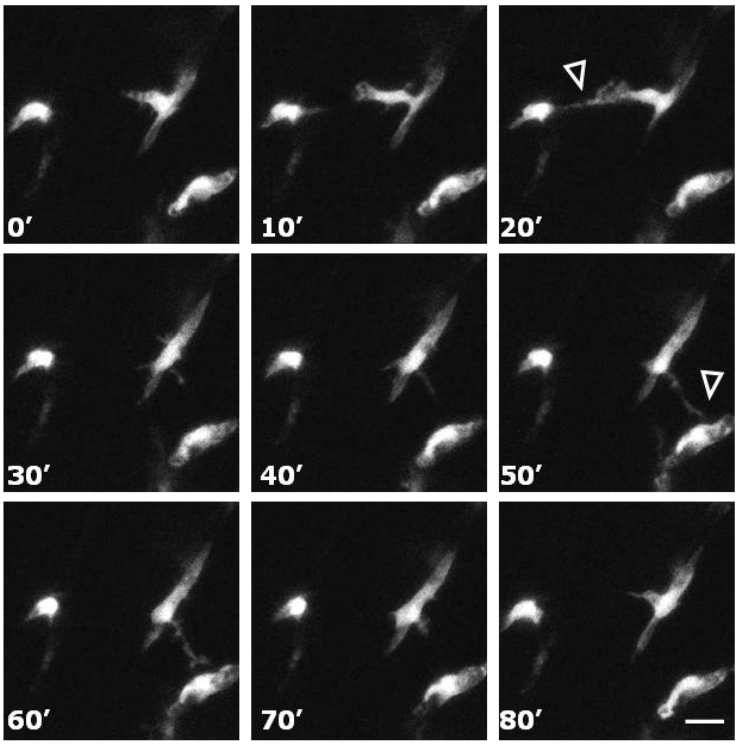

Figure 9. Microglia making contact.
A. Two microglial cells making contact (arrowhead) with their somas during 90'. They subsequently migrate away from each other, keeping contact with a thin process. When they finally let go (140'), another cell starts making contact with different processes (arrowheads in 160' and 170'). **B.** Three microglial cells, of which the middle one first reaches out a protrusions and contacts the microglial cell in the left (20', arrowhead) and then sends out another process to contact the cell in the right (50', arrowhead). Images are cropped Z-projections (10 optical slices with a z-step of 8µm) from the E15.5 time-lapse movie. ', minutes. Scale bar= 20µm in all micrographs.

We demonstrated that microglia at E14.5 migrate at a mean velocity of 0.57 ± 0.04 µm/min, which was similar to the migration velocity at E15.5 (0.54 ± 0.04 µm/min) **(Fig. 10)**. The highest migration velocities for E14.5 and E15.5 were 1.96 µm/min (117.54 µm/h) and 0.77 µm/min (46.02 µm/h) respectively. A few studies have investigated the dynamics of microglia in mammalian live brain slices during postnatal development (51, 52) and some during adulthood (11, 53). Stence et al. used P3-P14 rats to study the effect of tissue slicing on the activation of these cells. They established that ramified microglia rapidly activated, and changed morphology to migrate up to 1.97 µm/min (118.2 µm/h), as a response to the tissue slicing (51). However, Stence et al. dissected out the hippocampi and used a manual tissue chopper to section the tissue. The dissection and slicing technique could have induced significant tissue damage and consequently a higher microglial response to the injury. Moreover, they started recording time-lapse videos within 60-75min of decapitation, while we first let the slice equilibrate and started recording within 3-4h of decapitation. In addition, it could be possible that the authors recorded starting at the cutting surface of the slice, while we measured deep into the slice, to image the non-activated microglial population. Carbonell et al. performed time-lapse imaging on stab-lesion injured adult mouse brains using the same dissection and slicing methods as we did (53). They concluded that the slicing procedure itself did not acutely induce significant migration of microglia. Moreover, the microglial morphology in our time-lapse movies closely resembled the morphology of microglia in our fixed sections, so we can assume that the microglia we imaged during time-lapse experiments did not undergo significant changes in activation stage.

As appears from the colored migration tracks in **Fig. 11-A** and Suppl. fig. 7 and 8, microglia at E14.5 and E15.5 move in very distinct individual manners. Some cells migrated long distances, while others stayed more or less on the spot. The same microglial cell could migrate in all directions: forward, backward and sideways. After analyzing microglial migration tracks, absolute

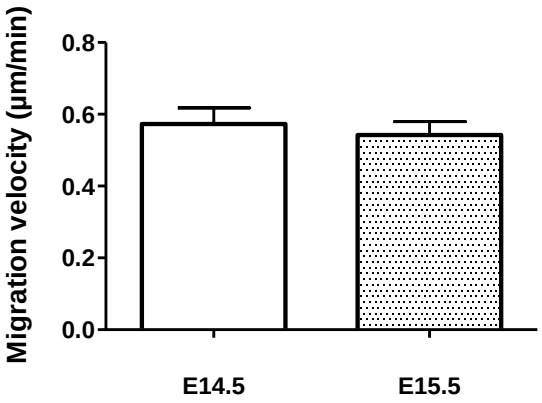

Figure 10. Migration velocity of microglia in the E14.5-E15.5 neocortex. At E14.5, microglia migrate at a mean velocity of 0.5733 µm/min (or 34.4 µm/h) (n=41). At E15.5, the mean migration velocity is 0.5427 µm/min (or 32.6 µm/h) (n=15). Means ± SEM are indicated. Mann Whitney test was applied.

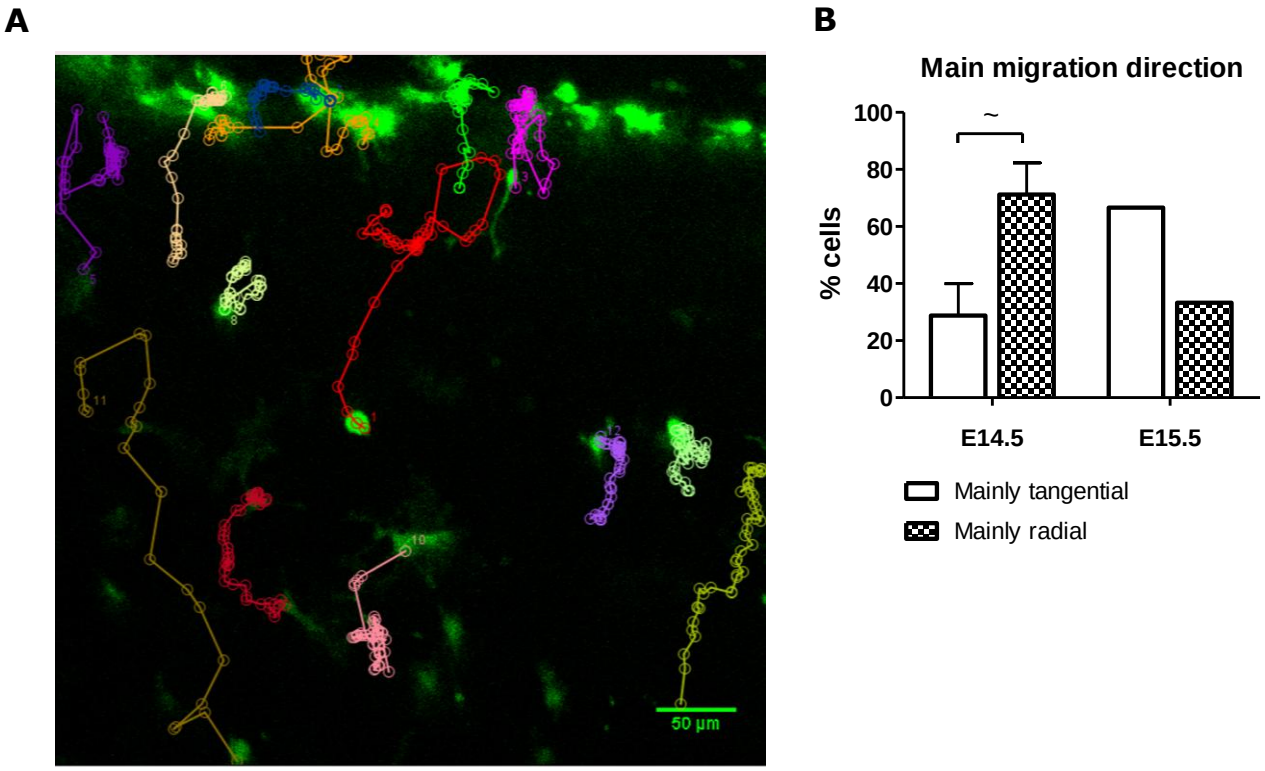

Figure 11. Migration of microglia in the E14.5-E15.5 neocortex. Acute coronal brain slices were live imaged during 7 hours by means of multi-photon excitation microscopy and microglial migration was tracked using MTrackJ in ImageJ. **A.** Microglial migration pathways in the E14.5 neocortex of 1 experiment. Colored connected points represent the location of the microglial soma at each time point and track numbers indicate the last time point. The pia is located on top, marked by the high density of bright fluorescent microglia. Note that some cells migrate longer distances than others and move in different fashions. **B.** Main migration direction of E14.5 and E15.5 microglia. Absolute migrated distance between successive time points in X (tangential direction) and Y (radial direction) coordinates was calculated per cell. The main migration direction was considered tangential if the sum for X was higher than the sum for Y and the other way round. Microglia tend to migrate more radially than tangentially in the E14.5 neocortex (N=3) and more tangentially in the E15.5 neocortex (N=1). Means ± SEM are indicated. Mann Whitney test (B) was applied and ~=p<0.1.

migrated distances between successive time points were calculated per cell in the X (tangential) and Y (radial) coordinates (see Suppl. table 1 for raw data). To determine the main direction the cells were migrating, the absolute distances were summed up per coordinate. If the sum for X was higher than the sum for Y, the main direction was considered tangential, otherwise it was considered radial. **Fig. 11-B** shows a trend towards more mainly radially than tangentially migrating microglia at E14.5 (71.17 ± 11.13% versus 28.83 ± 11.13%) ($p<0.1$). However, at E15.5, this trend was reversed. 66.66% of the total microglia migrated mainly tangential while 33.33% migrated mainly radial. The higher percentage of mainly tangentially migrating cells could be related to the field of imaging. At this age, the neocortex consists of three morphologically well-distinguishable regions, namely the ventricular zone, the intermediate zone and the cortical plate. Since the cortical surface at E15.5 becomes much larger than the ventricle, radial fibers that span the neocortex follow a long ventrolateral course through the intermediate zone and then turn to extend radially through the cortical plate to the pia (54). Consequently, the intermediate zone exhibits a tangential orientation of radial fibers and cellular bodies **(Fig. 17-,19-, and 20-D2)**. Since at E15.5 the neocortex becomes too wide, it is not feasible to image the entire thickness of the neocortex, so possibly a part of the intermediate zone was situated in the imaging field.

As appears from a 3-D reconstitution of individual migration tracks **(Fig. 12)**, microglia did not migrate in only one plane, but they also moved throughout the Z-direction (depth of the slice), matching the rostral-caudal direction in the embryonic brain. Tracks from 3 different microglia were chosen as examples to discuss. **Fig. 12-A** shows the track of a microglial cell migrating at a velocity of 1.05 µm/min (and which travelled a long distance). This track corresponds to track 1 (red) in **Fig. 12-A.** The microglial cell first migrated in the tangential direction, after which it made a turn of 360° to migrate mainly radial. In addition, this cell migrated from rostral to caudal in the neocortex. In **Fig. 12-B** the track of a cell with an intermediate migration velocity (0.65 µm/min) (and which travelled an intermediate distance) is plotted. This track matches track 6 (pink) in Suppl. fig. 7-A. The cell migrated in a zigzag pattern from the pia into the parenchyma, while migrating from caudal to rostral. Moreover, when moving along the rostral-caudal axis, the cell sometimes moved back and forth. **Fig. 12-C** shows the path of a slow moving microglial cell (0.41 µm/min) (and which travelled a short distance), which corresponds to track 10 (white) in Suppl. fig. 7-B. This cell migrated scarcely in the radial or tangential direction, it only travelled from rostral to caudal. So, the term "locomotion" is more appropriate for the movement of this cell. Microglia which migrated long distances were automatically characterized by a higher velocity, since the total migrated length per cell was used to calculate velocity.

The microglial migration tracks in the neocortex suggest that these cells do not move in the same uniform direction. Instead, they seem to follow individual routes on which they move sideways, forwards and backwards and along the rostral-caudal axis. However, the cells do move in a general stream. At E14.5, the intermediate zone has not developed to the same extent as at E15.5, so the radial processes follow a more general radial course throughout the neocortex than at E15.5, where the radial course of the fibers is interrupted to some extent by the tangentially oriented fibers in the intermediate zone. In this way, we found that microglia at E14.5 tend to migrate more radially than tangentially. These results correspond to the results from the fixed analysis in **Fig. 8-A**, which also shows a trend towards more processes oriented radially at E14.5. However, the

orientation of the main migratory stream at E15.5 was tangential, leading us to presume that the intermediate zone was in the field of imaging. If this actually was the case, it could be suggested that the orientation of microglial migration can be influenced by the local course of the radial fibers. However, no proper conclusions could be drawn from the results on E15.5, since the imaged area of the neocortex could not be identified.

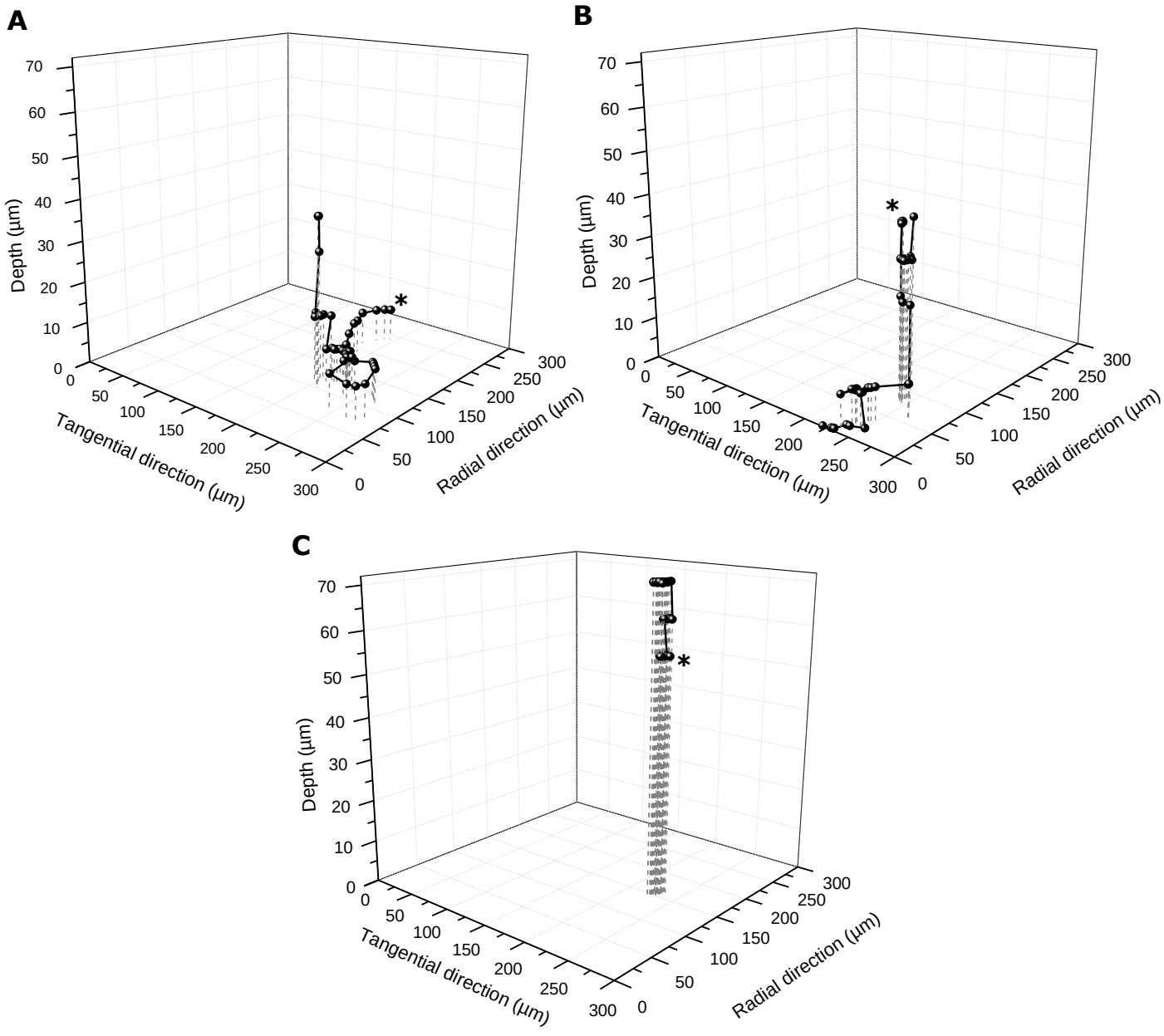

Figure 12. 3-Dimensional representation of 3 different microglial migration tracks. X,Y and Z coordinates of microglial migration tracks were plotted into 3-D graphs in OriginPro 8. **A.** Track of a fast migrating cell (62.82 µm/h). **B.** Track of a migrating cell with intermediate velocity (38.7 µm/h). **C.** Track of a slow migrating cell (24.3 µm/h). Note that microglia migrate not only in one plane, but also in the Z-direction, thus along the rostral-caudal axis of the neocortex. 70µm depth corresponds to rostral, while 0µm depth is located caudally. Ending points of the migration tracks are indicated with an asterisk.

Subsequently, the migrated distance (µm) between successive time points was plotted in function of the time (h), in order to view the pattern of migration **(Fig. 13)**. The three microglial cells from **Fig. 12** were taken as an example. All migration patterns were spiked, so microglial movement does not occur continuously, but is characterized by phases of active migration interspersed with stationary phases. This pattern was previously described in neurons that adopt glia-guided locomotion as saltatory locomotion (55). These neurons sent out a short leading process, as most microglia did in our time-lapse experiments, in comparison to neurons that moved by means of somal translocation (55). In this way, it is tempting to speculate that the pattern of locomotion is affected by the substrate the migrating cell is using/following.

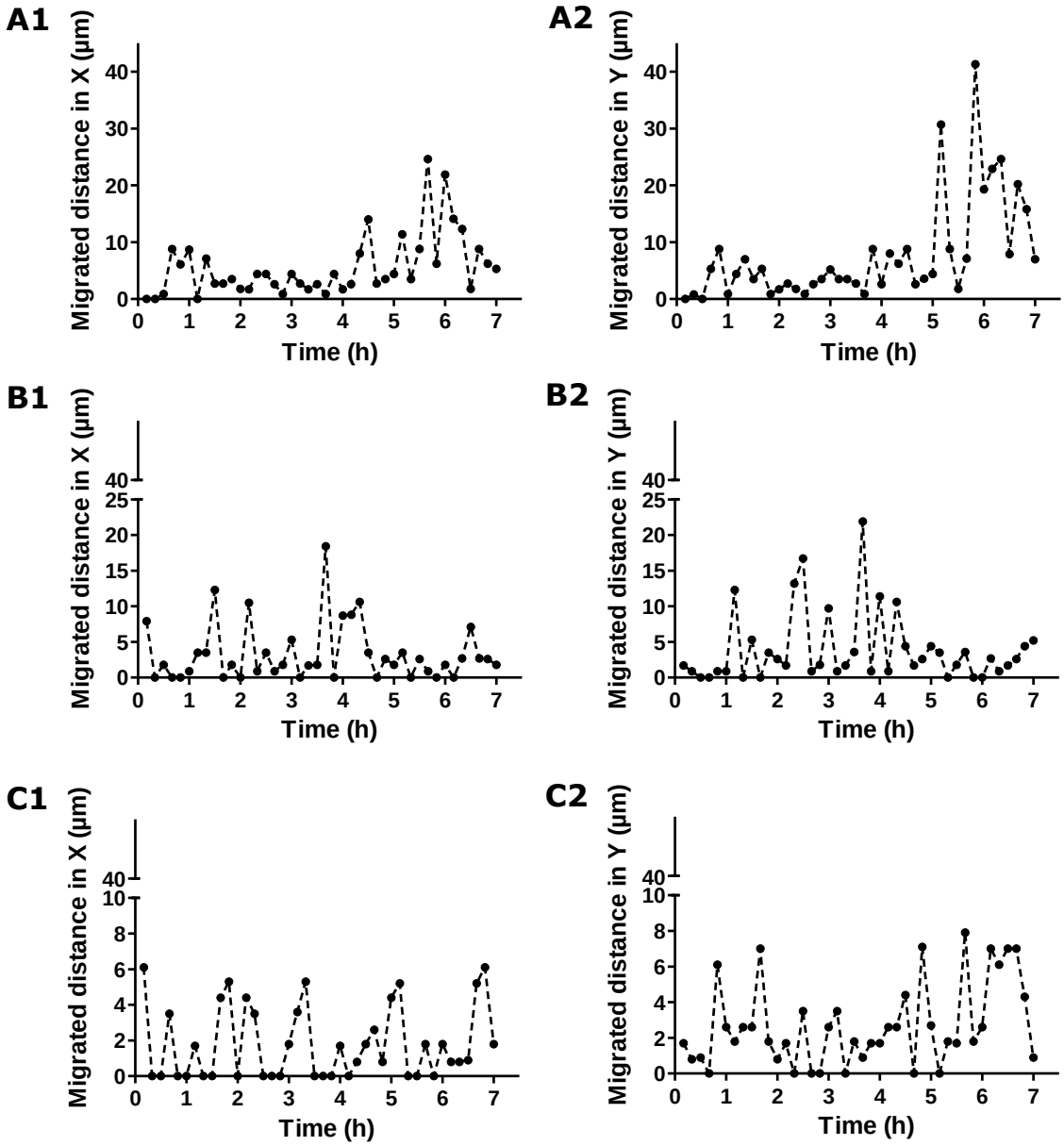

Figure 13. Microglial migration patterns. Absolute migrated distance between successive time points in X (tangential direction, **A1,B1,C1**) and Y (radial direction, **A2,B2,C2**) coordinates was calculated per cell and plotted on a timescale. Patterns in **A** are derived from the cell in Fig. 12A (high velocity of migration); **B** from Fig. 12B (intermediate velocity) and **C** from Fig. 12C (low velocity). Note that the migration patterns are spiked, meaning that microglial migration is characterized by phases of locomotion interspersed with stationary phases (migrated distance=0).

In the time-lapse movies, we observed that during the stationary phases, microglia sent out multiple protrusions, with some ending in lamellipodia and of which the shape was constantly being adapted (every 10 minutes). When the cells started to migrate for longer distances, they transformed into uni- or bipolar cells, sending out one leading process, which varied in length and thickness. Subsequently, the nucleus was translocated and the rear of the cell was retracted. **Fig. 14-16** show the microglia (every 30 minutes) of which the migration tracks were plotted in **Fig. 12.** The morphology of the fast migrating microglia **(Fig. 12-A)** is visible in **Fig. 14**. The microglial cell sent out multiple thin and broad processes and lamellipodia, changing every 10 minutes. At 4.5h, the cell achieved a bipolar morphology with broad protrusions and started to migrate for a longer distance. In addition, the nucleus became flattened while the cell was migrating. **Fig. 15** shows the microglial cell with an intermediate migration velocity **(Fig. 12-B)**, which migrated out of the pia into the neocortex. From 0-1.5h, the cell was located in the pia. Next, it migrated out of the pia, exhibiting a flattened bipolar morphology with short, broad extending processes. At 4.5h, the cell started contacting a nearby microglial cell. When the contact had ended, the cell sent out thin, scanning processes. **Fig. 16** depicts the morphology of the microglial cell migrating with a low velocity **(Fig. 12-C)**. From 0-2h the microglial cell exhibited one to three thin processes. At 2h, it had translocated its nucleus, with subsequent retraction of the process being behind. From that moment on, the cell stayed rounded with very subtle changes in morphology and did hardly migrate any further. Therefore, the pattern related more to locomotion than to migration.

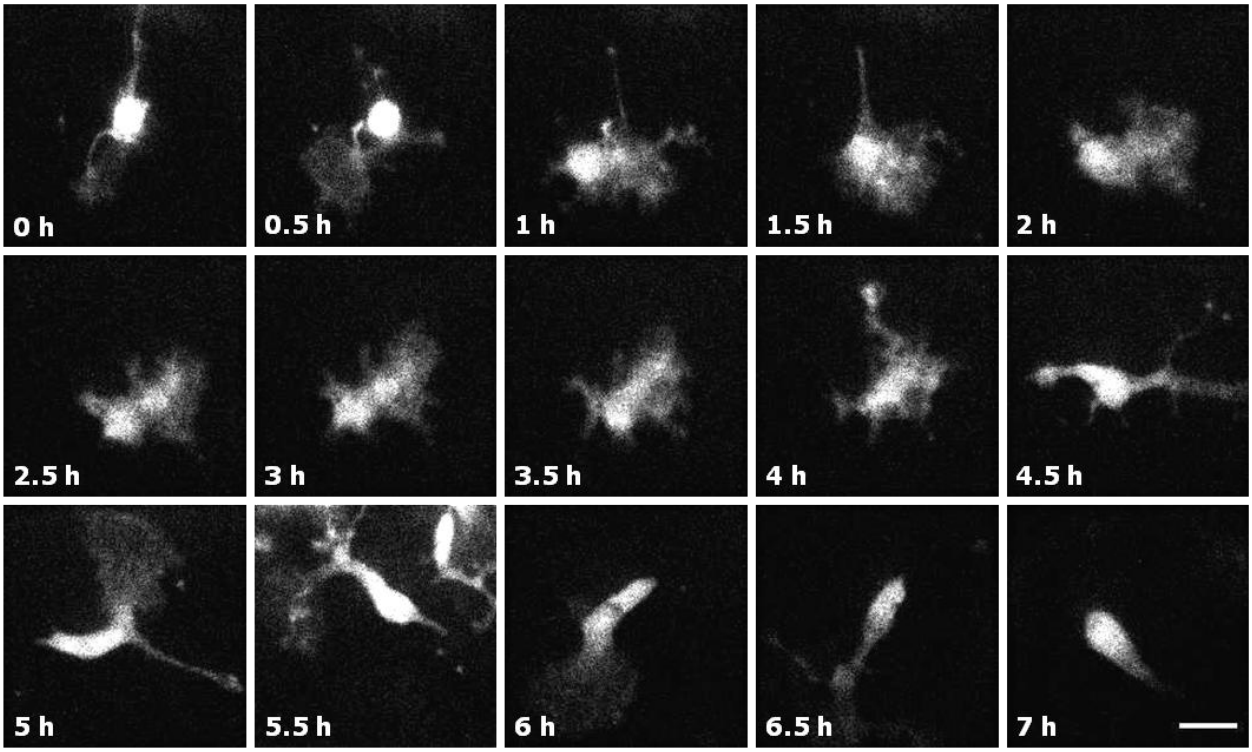

Figure 14. Changing morphology of a fast migrating microglial cell. This cell matches to the one in Fig. 12-A. The microglial cell sent out multiple long, thin and short, broad processes and lamellipodia, reshaping every 10 minutes. At 4.5h, the cell achieved a bipolar morphology with broad extended processes and started to migrate for a longer distance, while regularly forming broad lamellipodia. The nucleus became flattened while the cell was actively migrating. Images are cropped Z-projections (10 optical slices with a z-step of 8µm) from the time-lapse movie. Scale bar=20µm in all micrographs.

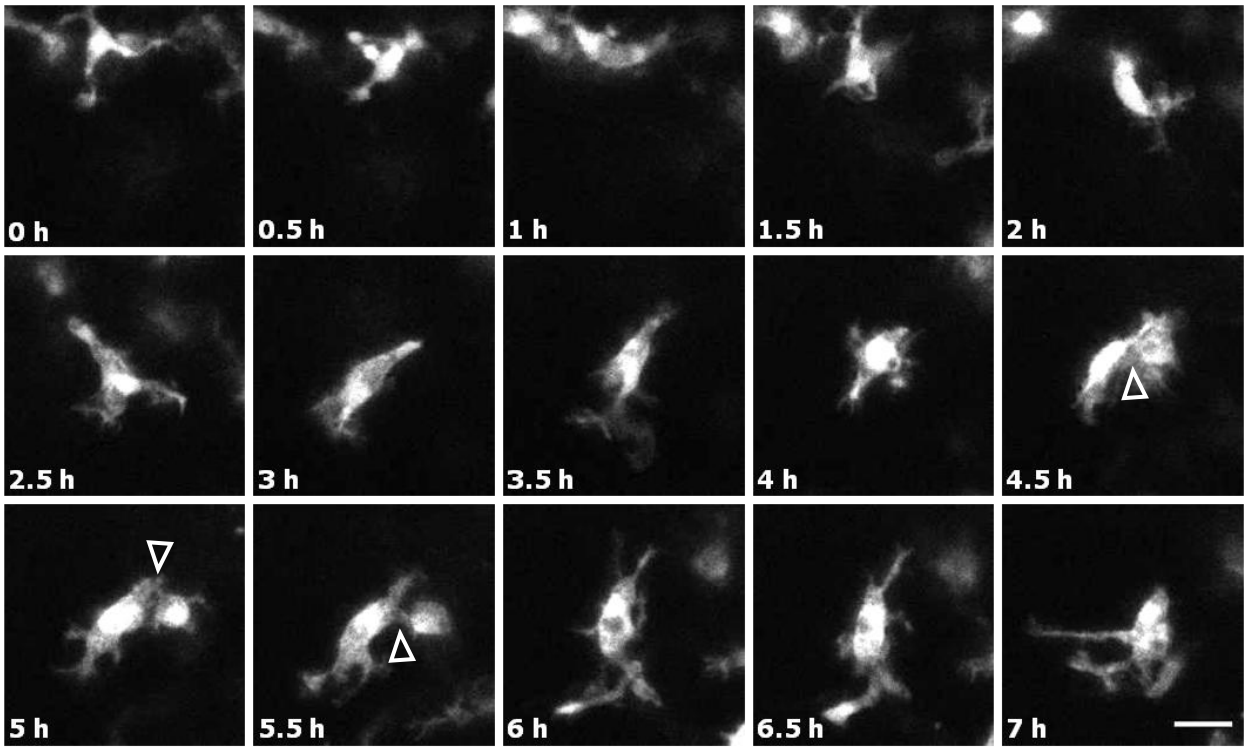

Figure 15. Changing morphology of a migrating microglial cell with intermediate velocity. This cell matches to the one in Fig. 12-B. From 0-1.5h, the cell was located in the pia. Next, it migrated out of the pia, exhibiting a flattened bipolar morphology with broad extending protrusions. At 4h, the cell became rounded and started contacting another microglial cell (arrowheads). When the contact had ended, the cell sent out thin, scanning processes. Images are cropped Z-projections (10 optical slices with a z-step of 8µm) from the time-lapse movie. Scale bar=20µm in all micrographs.

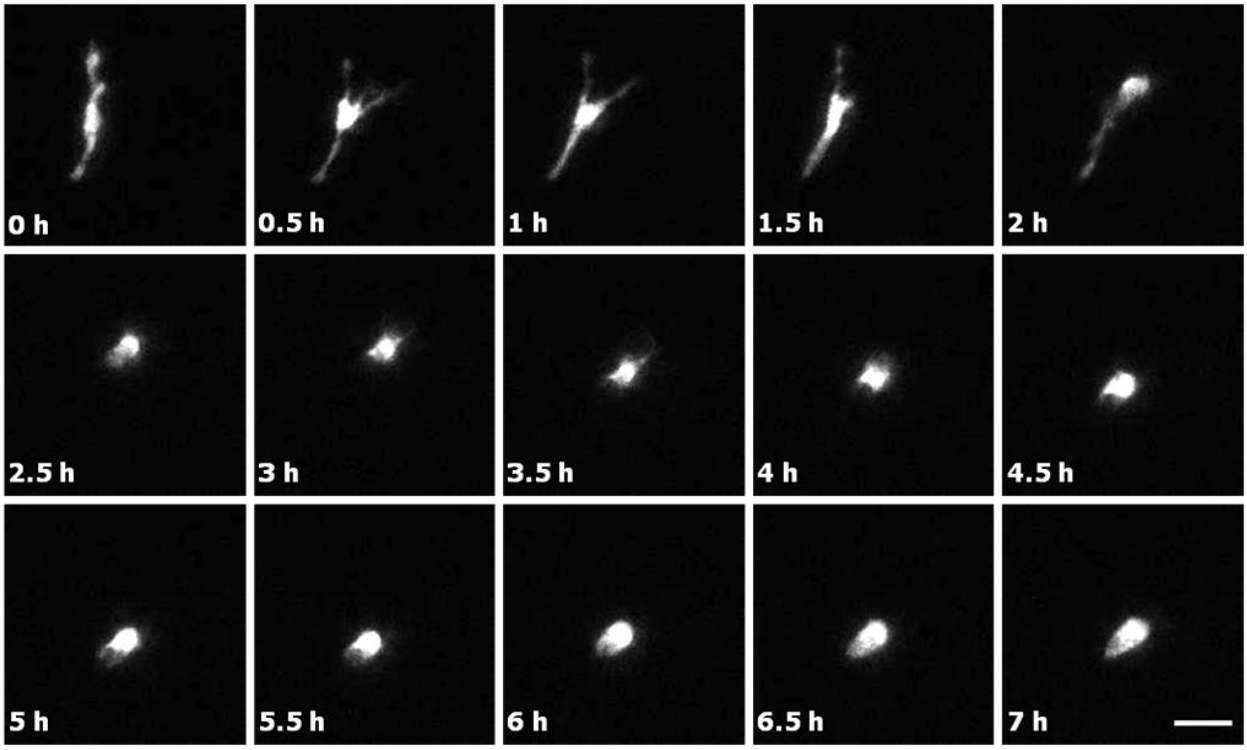

Figure 16. Changing morphology of a slow migrating cell. This cell matches to the one in Fig. 12-C. From 0-2h the microglial cell exhibited one to three thin processes. At 2h, it had translocated its nucleus, with subsequent retraction of the rear. From that moment on, the cell stayed rounded with very subtle changes in morphology and showed some on spot locomotion. Images are cropped Z-projections (10 optical slices with a z-step of 8µm) from the time-lapse movie. Scale bar=20µm in all micrographs.

Cellular mechanisms for tangential and radial microglial migration were previously studied in the embryonic quail retina by means of immunohistochemical stainings (36, 37). The mechanism for tangential migration in the retina involved polarized emission of lamellipodia at the leading edge of the cell, strong cell-to-substrate (Müller cell end-feet) attachment, translocation of the cell body forward, and retraction of the rear of the cell (36). Furthermore, other amoeboid cells were multipolar, with lamellipodial projections radiating in all directions from the cell body. Microglia in the process of radial migration in the retina first emitted a leading process directed toward the next retinal level. Then, the nucleus translocated along the leading process, reaching its end at the next level, while the end of the leading process ramified. Finally, the rear process retracted. In contrast to tangential migration, no lamellipoda were observed during radial migration (37). In our time-lapse experiments, we observed microglia migrating with the same characteristics as described in both types of migration in the retina. This indicates that the modes of microglial migration in the embryonic neocortex are more heterogeneous, than the well-distinguishable forms in the retina. This heterogeneity can in turn be related to the complexity of the tissue the cells are located in (the retina shows a highly structured laminar organization). Furthermore, Lee at al. examined the resting microglial behavior in the developing mouse retina (P0-P21) and remarked that developing microglia exhibited similar patterns of process motility as microglia of the adult retina, indicating that dynamic microglia behavior is a property of developing and mature systems (56). When taking the time-lapse data into consideration, it is likely that the results of the fixed analysis (section 3.1) are not a fully suitable representation or prediction for the orientation of the general migratory stream, since microglia constantly adapt the multiple protrusions they send out in several directions during the stationary phases. These directions do not necessarily correlate with the direction of migration they will adopt. In other words, the microglia in the embryonic neocortex first seem to scan their environment for possible cues, before deciding which direction to migrate.

All together, the time-lapse data imply that embryonic microglia located in the neocortex are dynamic cells, which constantly scan the environment with multiple orientated processes and which make contact with each other on a regularly basis. Their migration tracks are quite heterogenous, as microglia move along individual tracks instead of collective patterns. Based on the nestin labeling from the fixed analysis (contact between microglia and radial processes) and the microglial migration tracks, these cells could make successive jumps between pillars of radial fibers. We next investigated the presence of adhesion molecules (laminin, LMR, fibronectin, FNR) on radial cells and microglia, which could be involved in during the contact between radial cells and microglia.

3.3 Expression of adhesion molecules in the embryonic neocortex

To determine the presence of adhesion molecules on microglia and radial cells, fixed E12.5-E15.5 coronal brain sections were double-immunostained. Labeling for nestin was always performed in combination with staining for one of the following molecules: the ECM glycoproteins laminin and fibronectin, and their receptors α6 integrin and α5 integrin. All stainings were performed on 10µm thick embryonic coronal sections of the neocortex ranging from rostral to caudal. Stainings were photographed using a wide-field fluorescence microscope in order to study the expression patterns.

Confocal images were taken in order to visualize both stainings (A555 and A647). The DAPI channel was omitted to retain the clarity of the pictures.

3.3.1 Laminin is present on radial cells, according to a specific spatiotemporal pattern

Laminin is a cruciform ECM glycoprotein which contains an α, β, and γ chain. These molecules are able to modulate differentiation of epithelial cells, neurite outgrowth, anchoring of epidermal basal cells, and anchoring of leukocytes that are exiting from the microvasculature. In addition, laminins are important components of basement membranes (43).

Fig. 17 shows the double labeling for laminin (in red) and nestin (in purple) ranging from E12.5-E15.5. Nestin is clearly expressed by radial cells **(Fig. 17-B2 and D2)**. Laminin is expressed as punctuate deposits throughout the neocortex. In addition, the pia together with blood vessels were highly positive for this ECM protein. On E12.5, the typical punctuate deposits were most pronounced. Their expression pattern was the same from rostral to caudal. The inferior part of the neocortex (the part adjacent to the GE) showed a clear point staining towards the pia and halfway up, laminin dots were present towards the ventricular lining (not shown). In this way, the more superior part of the neocortex harbored laminin expressing in a fine, radial pattern **(Fig. 17-A1)**. A merge of the two stainings revealed a perfect co-localization of the laminin points on the radial fibers, suggesting that laminin is produced by radial cells in the mouse embryonic neocortex **(Fig. 17-A3-D3)**. At E13.5, rostrally the point staining becomes very weak. More caudally (near the GE), the laminin points are still detectable, but have clearly diminished and are now only present half way the cortex, near the pia **(Fig. 17-B1)**. At E14.5, the expression fades away even more **(Fig. 17-C1)**, so that only the very superior part of the neocortex shows a light point staining. Until now, laminin expression stays evident near the pia in the developing corpus callosum (not shown). At E15.5 the punctuate laminin deposits seem to have disappeared, in such a way that the expression becomes restricted to only the pia and blood vessels **(Fig. 17-D1)**. Microglia (green) contacting the nestin positive radial fibers with their processes can be viewed in all the zoom+merge images (area from white frame).

The laminin expression pattern we observed concurs with the distribution shown by previous studies. In the developing rat brain (E8-21), Liesi found that punctuate laminin deposits exhibited a specific spatiotemporal expression and that they were present along radial fibers (stained by vimentin) (40). Laminin immunoreactivity was also described by Liesi in the developing mouse optic and corpus callosum (39). The author speculated on a role for laminin in mediating neuronal-glial interactions and directing neuronal migration and promoting axon elongation (39, 40).

See next page **Figure 17. Laminin and nestin expression in the embryonic neocortex.** Confocal images of coronal CX3CR1$^{+/eGFP}$ mouse brain sections. Microglia expressing eGFP (green), laminin (A555-red) **(A1-D1)** and nestin (A647-purple) **(A2-D2)** double staining in the E12.5-E15.5 neocortex. **A3-D3** represent a 4x digital zoom and fusions of the area indicated by the white frame. Laminin is expressed as fine punctuate deposits on radial glial fibers. As the embryo ages, laminin expression remains restricted to the pia and blood vessels (highly positive round and elongated structures). N=3 for all ages. A microglial precursor was present inside a blood vessel (D1,arrowhead). Scale bar=20μm, except for Zoom+merge images (scale bar=10μm).

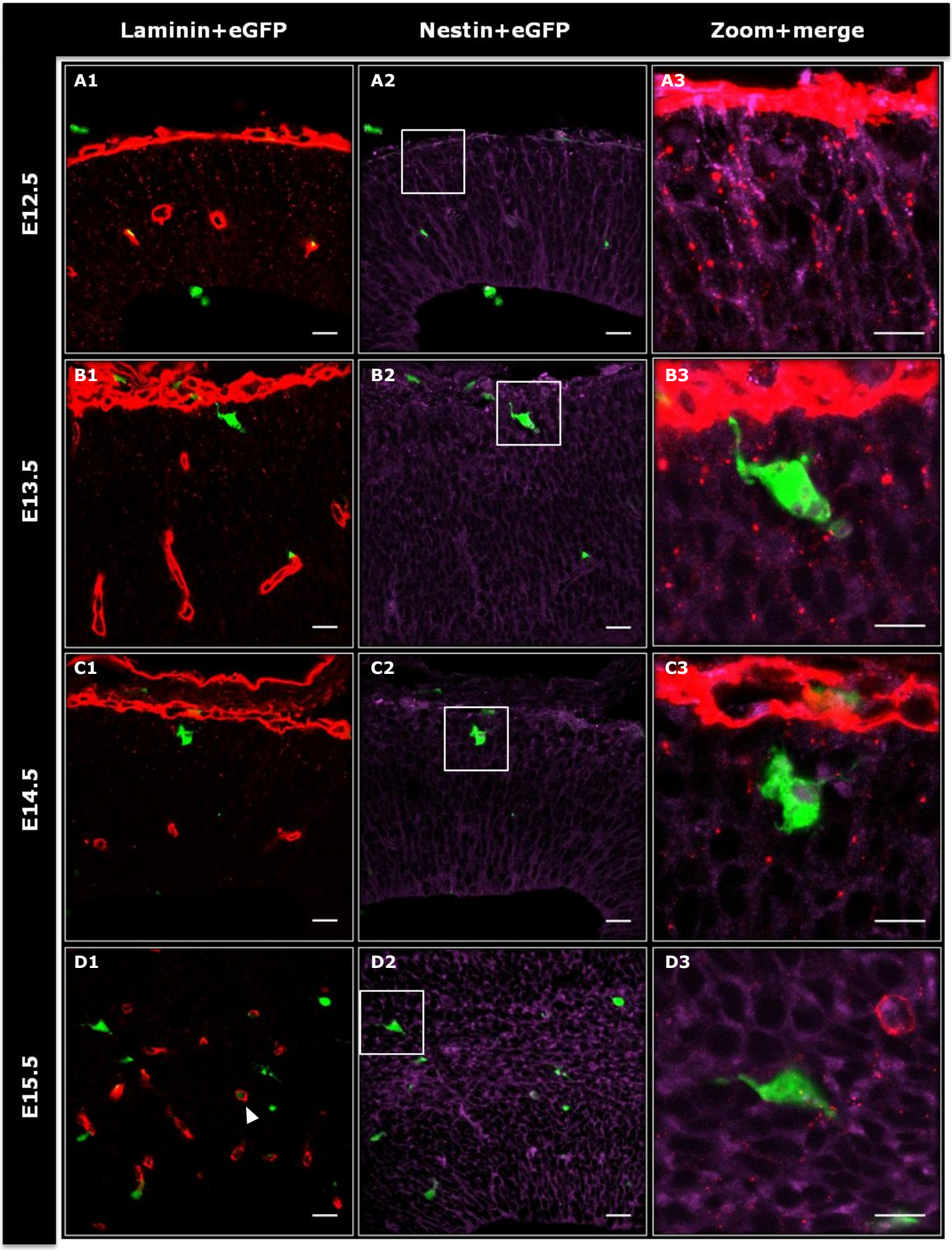
Laminin+eGFP
Nestin+eGFP
Zoom+merge
E12.5
E13.5
E14.5
E15.5
A1
A2
A3
B1
B2
B3
C1
C2
C3
D1
D2
D3

3.3.2 Microglia and radial cells express the laminin receptor

Adhesion to laminin is regulated via the laminin receptor. As all other integrins, this receptor consists of an α- and β-subunit. To form the LMR, several α-subunits can dimerize with the β1-subunit (57). However, Milner et al. proved that the α6β1 integrin was highly expressed by cultured microglia from postnatal mice (P0-P2) and that this was the major functional receptor expressed by microglia (44). Therefore, we used the same α6 monoclonal antibody (GoH3) to identify this subunit, *in situ* in embryonic brain sections.

Fig. 18 shows the double labeling for α6 integrin (in red) and nestin (in purple) ranging from E12.5-E15.5. We observed that from E12.5-E15.5 (rostral to caudal) the α6-subunit was homogenously expressed throughout the entire thickness of the neocortex in a radial pattern, although its staining intensity weakened slightly with increasing embryonic age **(Fig. 18-A1-D1)**. As appears from the confocal images in **Fig. 18-C1 and D1**, the antibody did not always succeed to optimally penetrate the tissue (wide-field fluorescence images confirm that the expression is homogenous). Furthermore, blood vessels were also weakly stained by this antibody (open arrowheads in **Fig. 18-A1 and C1**). When the two labelings are merged **(Fig. 18-A3-D3)**, the homogenous staining becomes co-localized with the nestin positive radial fibers, as the fibers now color completely pink. When zoomed in on the microglia (green), especially their protrusions are highly positive for the LMR (yellow, filled arrowheads). Suppl. fig. 9 depicts the imprints of the microglial protrusions in the LMR staining clearly, as the nestin channel is omitted and eGFP and α6 channels are shown separately. Amoeboid microglia in the ventricle lumen are highly positive for the LMR **(Fig. 18-B1,C1 and D1)**. The co-localization indicates that radial cells and microglia express the LMR. Microglia contacting the nestin positive radial fibers with their processes can be viewed in all the zoom+merge images (area from white frame).

Our results correspond to the findings of Whitley et al. in the olfactory bulb of embryonic (E13-E17) mice. They observed that α6 integrin, implicated in neuronal migration, is expressed in radially oriented patterns extending from the VZ to the superficial layers and colocalizes with radial cells (stained by RC2). This pattern was consistent at all embryonic ages examined. Blood vessels and the pial surface were also immunoreactive (58). Moreover, we confirm that the findings of Milner et al. concerning the *in vitro* expression of the LMR by postnatal cultured microglia, apply also to the embryonic microglia *in situ* (44). The immunoreactivity suggests that microglia can interact with laminin, produced by the radial cells of the neocortex from E12.5-E15.5

See next page **Figure 18. α6 integrin (LMR) and nestin expression in the embryonic neocortex.** Confocal images of coronal CX3CR1$^{+/eGFP}$ mouse brain sections. Microglia expressing eGFP (green), α6 integrin (A555-red) **(A1-D1)** and nestin (A647-purple) **(A2-D2)** double staining in the E12.5-E15.5 neocortex. **A3-D3** represent a 4x digital zoom and fusions of the area indicated by the white frame. α6 integrin is homogenously expressed along radial glial fibers. Microglial protrusions are positive for the LMR (yellow color, filled arrowheads). Amoeboid microglia in the ventricular lumen show a higher expression of the LMR **(B1,C1,D1)**. The α6 integrin antibody also weakly stains blood vessels (open arrowheads). α6 integrin and microglia separate channel images can be consulted in Suppl. fig. 9. N=2 for E13.5, N=3 for other ages. Scale bar=20μm, except for Zoom+merge images (scale bar=10μm).

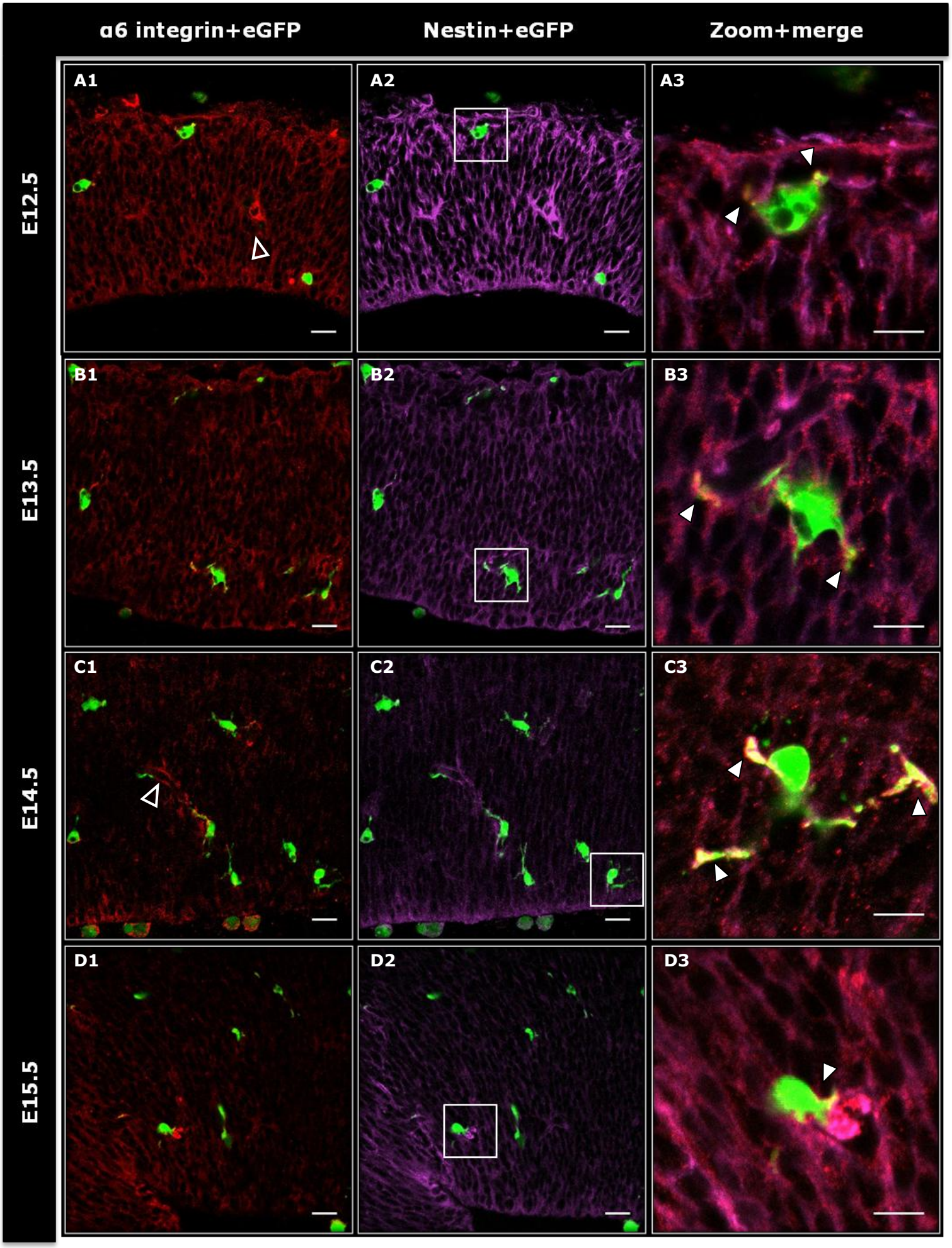
α6 integrin+eGFP
Nestin+eGFP
Zoom+merge
E12.5
E13.5
E14.5
E15.5
A1
A2
A3
B1
B2
B3
C1
C2
C3
D1
D2
D3

3.3.3 Fibronectin is present on radial cells in a homogenous pattern

Fibronectin is a heterodimeric multifunctional glycoprotein, which is abundant in the blood and in most tissues, where it assembles into fibrils that enhance cell adhesion. Furthermore, it has been shown to be implicated in cell migration and differentiation and to be essential for normal embryonic development (59). In addition, fibronectin is another important component of basement membranes (43).

Fig. 19 shows the double labeling for fibronectin (in red) and nestin (in purple) ranging from E12.5-E15.5. Fibronectin is present from rostral to caudal in a more diffuse pattern than laminin. The expression is not demonstrated as fine punctuate deposits, but rather as thick aggregates throughout the neocortex **(Fig. 19-A1-D1)**. From E12.5-E14.5 the fibronectin expression shows similar characteristics. However, at E15.5 the staining intensity slightly diminished and the intermediate zone exhibited a less dens staining pattern **(Fig. 19-D1)**. As appears from the confocal image in **Fig. 19-B1**, the antibody did not always succeed to optimally penetrate the tissue. When nestin and fibronectin channels were merged, the fibronectin expression clearly co-localized with the radial fibers **(Fig. 19-A3-D3)**, implicating that these cells produce the ligand in the embryonic neocortex from E12.5-E15.5. In addition, blood vessels were also marked by the fibronectin antibody (open arrowheads in **Fig. 19-B3 and C3**. Note the location of the microglial cells (green) in relation to the developing vasculature and to the radial fibers, to which they make contact.

In slight contrast with our observations, other studies have reported different expression patterns of fibronectin in the developing mammalian CNS. Immunohistochemical examination of the developing cerebral cortex from cats (E46-P7) revealed that fibronectin expression is restricted to the subplate and the marginal zones, and is not found in the VZ and CP (60). A study performed on the developing mouse neocortex (E10-E19) generated similar results (41). Fibronectin was expressed in a specific spatiotemporal pattern, with the ECM protein being present first at E11-E12 as small points in the preplate. Later, the staining was more diffuse in the preplate, marginal zone and subplate (E13-E14), but absent in the VZ. Starting from E18, fibronectin reactivity was restricted to blood vessels and the pia (41). Sheppard et al. did observe punctuate fibronectin deposits in the proliferative VZ of the developing mouse neocortex at E11 (42). At higher ages (E12 and E13), the fibronectin reactivity became restricted to the preplate and subplate. Finally, in correspondence with our results, they remarked that fibronectin closely associated with radial processes, but further study revealed that radial glia only produced the early fibronectin, when it was still present in the VZ, and that neurons, which are closely located to radial glia, were the predominant producers of fibronectin during migration in later stages of early cortical development (54). However in the developing chick optic tectum, the predominant source of fibronectin appeared to be radial glia and it was expressed diffusely throughout the entire neocortex (61).

See next page **Figure 19. Fibronectin and nestin expression in the embryonic neocortex.** Confocal images of coronal CX3CR1$^{+/eGFP}$ mouse brain sections. Microglia expressing eGFP (green), fibronectin (A555-red) **(A1-D1)** and nestin (A647-purple) **(A2-D2)** double staining in the E12.5-E15.5 neocortex. **A3-D3** represent a 4x digital zoom and fusions of the area indicated by the white frame. Fibronectin is expressed as dense punctuate deposits along radial glial fibers and on the pia and blood vessels (open arrowheads). N=3 for all ages. Scale bar=20µm, except for Zoom+merge images (scale bar=10µm).

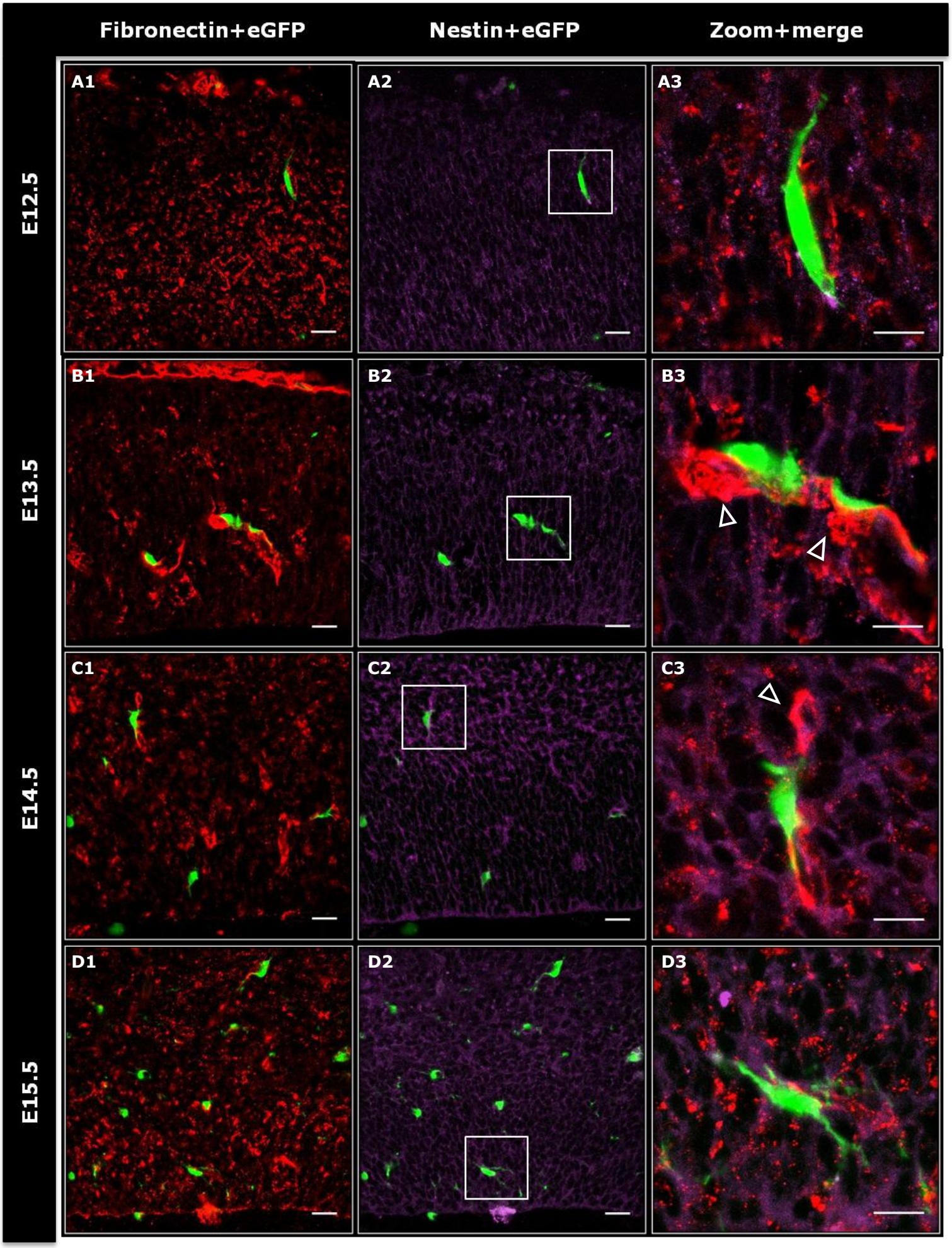
Fibronectin+eGFP
Nestin+eGFP
Zoom+merge
E12.5
E13.5
E14.5
E15.5
A1
A2
A3
B1
B2
B3
C1
C2
C3
D1
D2
D3

3.3.4 Radial cells express the fibronectin receptor as fine dots, microglia show a very weak expression

Adhesion to fibronectin is regulated through the fibronectin receptor, which is formed by the α5 integrin subunit together with the β1 chain (57). This integrin subunit is required during embryonic development as shown by the fact that mice lacking this subunit fail to develop and die around day E10.5 (62). In addition, Milner et al. showed that cultured microglia from postnatal mice (P0-P2) expressed α5β1 integrin (45). Since α5 exclusively dimerizes with the β1 chain, we used a monoclonal antibody against the α5 subunit to identify the FNR *in situ* in embryonic brain sections (57).

Fig. 20 shows the double labeling for α5 integrin (in red) and nestin (in purple) ranging from E12.5-E15.5. This staining showed a low expression of the FNR in the neocortical parenchyma, but obviously stained blood vessels. Expression patterns do not differ between rostral and caudal sections nor between embryonic ages **(Fig. 20-A1-D1)**. Again, the antibody did not always optimally penetrate the tissue **(Fig. 20-A1 and C1)**. The α5 integrin is not homogenously expressed in the embryonic neocortex, as the expression exhibits more a fine point labeling pattern. These fine α5 integrin points become more obvious in the merged zoom pictures **(Fig. 20-A3-D3)** and they seem to co-localize with radial fibers. Suppl. fig. 9 shows the separate channels for eGFP and α5, and reveals a very vague expression by microglia. Furthermore, microglial/monocytic precursors - characterized by a lower eGFP expression, than microglia located in the parenchyma - were visualized inside blood vessels (open arrowheads in **Fig. 20-C3**).

A study by Yoshida et al. identified the presence of the α5 integrin subunit on nestin positive cells as punctuate foci of reactivity in the embryonic neocortex of nestin$^{eGFP/+}$ mice, which corresponds to our results (63). Furthermore, other evidence indicates that the FNR functions in the regulation of neural morphology and migration during murine cortical development (64). Milner et al. demonstrated that microglia express the FNR *in vitro* (45). However, the immunoreactivity we observed against α5 integrin on microglia *in situ*, was rather weak, but could suggest that microglia make use of the FNR-fibronectin interaction to adhere to radial cells.

See next page **Figure 20. α5 integrin and nestin expression in the embryonic neocortex.** Confocal images of coronal CX3CR1$^{+/eGFP}$ mouse brain sections. Microglia expressing eGFP (green), α5 integrin (A555-red) **(A1-D1)** and nestin (A647-purple) **(A2-D2)** double staining in the E12.5-E15.5 neocortex. **A3-D3** represent a 4x digital zoom and fusions of the area indicated by the white frame. FNR staining exhibits a more punctuate profile and is colocalized with nestin positive radial glial fibers. Blood vessels are stained clearly by the α5 integrin antibody. Microglial protrusions are weakly positive for the FNR (filled arrowheads). Microglial precursors were visualized inside blood vessels **(C3)** (open arrowheads). α5 integrin and microglia separate channel images can be consulted in Suppl. fig. 9. N=2 for E13.5, N=3 for other ages. Scale bar=20μm, except for Zoom+merge images (scale bar=10μm).

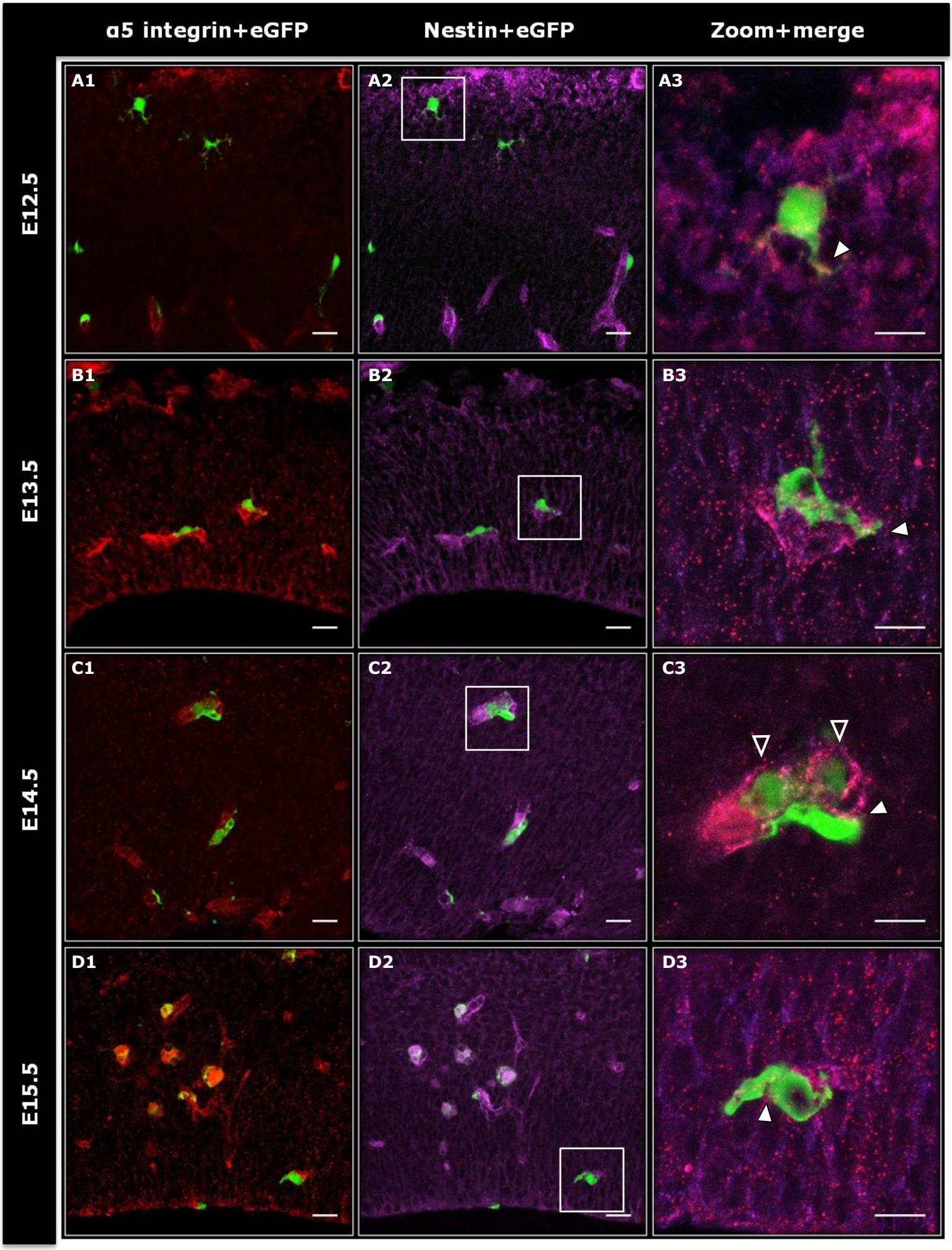
α5 integrin+eGFP
Nestin+eGFP
Zoom+merge
E12.5
E13.5
E14.5
E15.5
A1
A2
A3
B1
B2
B3
C1
C2
C3
D1
D2
D3

The immunohistochemical results from this project suggest that microglia are capable to interact with radial cells through the expression of receptors for the ECM ligands laminin and fibronectin, aligned by the latter. However, laminin does not seem to be ideally distributed in order to support microglial interaction throughout the entire neocortex. Taken into consideration the distribution of fibronectin, this ECM ligand is more likely to play a role in microglial adhesion to radial cells. Interestingly, the fibronectin expression pattern viewed here, differs from the one observed in other studies in the developing mouse neocortex (41, 42). For this project, we made use of an anti-mouse fibronectin antibody, while the former studies used antibodies direct against human fibronectin. So, this discrepancy in fibronectin distribution is not likely due to the studied animal species or embryonic age, but can be explained by the use of different antibodies, since the alternative splicing of pre-mRNA allows formation of multiple fibronectin isoforms (59). Since immunohistochemistry reveals that microglia express the FNR very weakly, other (more sensitive) detection techniques such as fluorescence-activated cell sorting (FACS) may be applied to detect α5 integrin expression on microglia from E12.5-E15.5. Furthermore, *in vitro*, microglia attached well to fibronectin substrates and weakly to laminin substrates (of which the adherence could be improved by administering cytokines), which indicates a functional interaction between microglia and the ECM (44).

In addition to serving as substrates for adhesion, laminin and fibronectin have been demonstrated to influence cultured embryonic (E17) rat microglia differentiation *in vitro* (65). When plated in the presence of fibronectin, microglia transformed into cells displaying a small soma and extending thin, long processes. Moreover, they lost the ability to phagocytose zymosan particles and showed a reduction in non-specific esterase activity and superoxide anion generation. In contrast, when laminin was added (even after incubation with fibronectin) the opposed effects occurred and the transformation to process-bearing microglia was inhibited. The spatiotemporal expression of laminin and the diffuse presence of fibronectin in the developing neocortex do not out rule the possibility that these ECM components might influence the differentiation of embryonic amoeboid microglia towards ramified cells. At E12.5, laminin is still present throughout the entire thickness of the neocortex, when the percentage of amoeboid cells is the highest compared to older embryonic ages **(Fig. 7-C)**. Laminin disappears gradually with increasing embryonic age, while also the amount of processes per microglia tends to increase (as a sign of ongoing differentiation) **(Fig. 7-B)**. Fibronectin immunoreactivity stays present in the neocortex, when laminin staining has already fully disappeared, excluding the reactivity in blood vessels and pia, which is also observed in the adult brain **(Fig. 17 and 19)**. In this way, laminin could keep the microglia in a more amoeboid form in the early embryonic neocortex, and inhibit the influence of the expressed fibronectin. Whether these ECM proteins could have an effect on the microglial production of (growth) factors that might influence in their turn neurodevelopmental processes, such as neuron survival, neurite outgrowth and synaptogenesis, remains an interesting question to investigate.

4 CONCLUSION AND SYNTHESIS

Previous studies and own preliminary results, led us to hypothesize that microglia in the developing neocortex migrate to their final destinations by making use of radial cells. By means of immunohistochemical stainings and live imaging, we aimed to elucidate (1) the migratory behavior of these brain macrophages and (2) the presence of adhesion molecules on microglia and radial cells, which could mediate attachment between these two cell types. To investigate these objectives, heterozygous transgenic CX3CR1eGFP mice embryos (E12.5-E15.5) were used in all experiments, in order to instantly visualize microglia.

We established that microglial location differed significantly between embryonic ages E12.5-E15.5, indicating that microglia until E12.5 concentrate near the pia and ventricular lining and from E13.5 start to colonize the intermediate layers of the neocortex. While dispersing throughout the nervous parenchyma, these cells increase their process length and tend to gain protrusions, which may indicate the start of differentiation towards ramified, scanning cells. At all ages, processes were randomly oriented in the neocortex, implying no significant preference for a specific migration direction. Moreover, microglial protrusions always made contact with radial processes.

By performing live imaging on E14.5 and E15.5 acute brain slices, we demonstrated that embryonic microglia in the neocortex are dynamic cells, which make contact with each other on a regularly basis. A general property was the constant scanning of the environment, by emitting and retracting multiple processes in various orientations. In this way, it seems that microglia first scan their environment for possible cues before deciding which direction to move. When microglia started to migrate, they retracted most processes and became uni-, bi- or tri-polar. They moved by first sending out a leading process, which varied in length and thickness. Secondly the nucleus was translocated and finally the rear of the cell was retracted, similar to the cellular mechanisms during microglial tangential and radial migration in the quail retina (36, 37). Embryonic microglia migrate at varied velocities (means on E14.5 and E15.5 were 0.57 and 0.54 µm/min), with some cells travelling long distances and other staying motile on the spot. These cells do not migrate in uniform patterns, but rather choose individual migration tracks. Microglial migration occurred not only in the X and Y direction, but also in the Z-direction, representing the movement along the rostral-caudal axis. Furthermore, movement was characterized by phases of locomotion interspersed with stationary phases, corresponding to the pattern of neurons adapting glial-guided locomotion (55).

Immunohistochemistry revealed the distribution patterns of the ECM proteins, laminin and fibronectin, and their receptors: α6 and α5 integrin subunits. Laminin was expressed as fine punctuate deposits along radial cells, according to a specific spatiotemporal pattern. At E12.5, laminin staining was evident, but having almost fully disappeared around E15.5. Fibronectin immunoreactivity was diffuse at each age and consisted more of punctuate aggregates, also being aligned along radial cells. Pia and blood vessels were intensely labeled for these molecules. LMR was homogenously expressed by radial cells and was also present on microglial protrusions. FNR was observed as fine points along radial cells and very weakly on microglia. These data suggest that microglia can adhere to ECM molecules present on radial cells. However, considering the

distribution patterns of the two ECM proteins, fibronectin seems more likely to support this interaction than laminin.

All together, our results imply that microglia are able to make contact with and can use radial cells during their migration to their final destinations in the neocortex, through expression of LMR and FNR. However, these cells do probably not solely follow the entire course of the radial cells. Instead, microglia could make successive jumps between pillars of radial fibers. Moreover, the often observed close association between microglia and blood vessels, could also postulate these structures as possible substrates for microglial migration.

To gain more insight into the essential substrates and molecular contacts for microglial migration, further research should focus on contact between microglia and partner cells and on the functional importance of adhesion reactions between microglia and radial cells and/or blood vessels. First of all, the expression of adhesion molecules in the developing neocortex should be extensively quantified. Contacts between microglia and other cells can be investigated by electron microscopy. Transgene mouse reporter models (for both microglia and radial cells/blood vessels) can be used to study the actual migration of microglia by means of live imaging. In this way, more information can be yielded concerning the used substrates. Furthermore, the function of integrins during microglial migration can be assessed by adding specific function blocking molecules in order to block migration. Further research will render more insight into the colonization of the neocortex by microglia, but still a long road lies ahead of us.

REFERENCES

1. Stiles J, Jernigan TL. The basics of brain development. Neuropsychol Rev. 2010 Dec;20(4):327-48.
2. Carlson BM. Human Embryology and Developmental biology. Third edition ed. Joanie M, editor. Philadelphia: Elsevier Mosby; 2004.
3. Verkhratsky A, Parpura V, Rodriguez JJ. Where the thoughts dwell: the physiology of neuronal-glial "diffuse neural net". Brain Res Rev. 2011 Jan 7;66(1-2):133-51.
4. Shibata T, Yamada K, Watanabe M, Ikenaka K, Wada K, Tanaka K, et al. Glutamate transporter GLAST is expressed in the radial glia-astrocyte lineage of developing mouse spinal cord. J Neurosci. 1997 Dec 1;17(23):9212-9.
5. Levitt P, Rakic P. Immunoperoxidase localization of glial fibrillary acidic protein in radial glial cells and astrocytes of the developing rhesus monkey brain. J Comp Neurol. 1980 Oct 1;193(3):815-40.
6. Gotz M, Huttner WB. The cell biology of neurogenesis. Nat Rev Mol Cell Biol. 2005 Oct;6(10):777-88.
7. Cooper JA. A mechanism for inside-out lamination in the neocortex. Trends Neurosci. 2008 Mar;31(3):113-9.
8. Marin O, Rubenstein JL. Cell migration in the forebrain. Annu Rev Neurosci. 2003;26:441-83.
9. Ginhoux F, Greter M, Leboeuf M, Nandi S, See P, Gokhan S, et al. Fate mapping analysis reveals that adult microglia derive from primitive macrophages. Science. 2010 Nov 5;330(6005):841-5.
10. Finlay BL, Darlington RB. Linked regularities in the development and evolution of mammalian brains. Science. 1995 Jun 16;268(5217):1578-84.
11. Nimmerjahn A, Kirchhoff F, Helmchen F. Resting microglial cells are highly dynamic surveillants of brain parenchyma in vivo. Science. 2005 May 27;308(5726):1314-8.
12. Chew LJ, Takanohashi A, Bell M. Microglia and inflammation: impact on developmental brain injuries. Ment Retard Dev Disabil Res Rev. 2006;12(2):105-12.
13. Garden GA, Moller T. Microglia biology in health and disease. J Neuroimmune Pharmacol. 2006 Jun;1(2):127-37.
14. Deverman BE, Patterson PH. Cytokines and CNS development. Neuron. 2009 Oct 15;64(1):61-78.
15. Chamak B, Morandi V, Mallat M. Brain macrophages stimulate neurite growth and regeneration by secreting thrombospondin. J Neurosci Res. 1994 Jun 1;38(2):221-33.
16. Bessis A, Bechade C, Bernard D, Roumier A. Microglial control of neuronal death and synaptic properties. Glia. 2007 Feb;55(3):233-8.
17. Stevens B, Allen NJ, Vazquez LE, Howell GR, Christopherson KS, Nouri N, et al. The classical complement cascade mediates CNS synapse elimination. Cell. 2007 Dec 14;131(6):1164-78.
18. Martin CB, Ingersoll SA, Martin BK. Transcriptional control of the C3a receptor gene in glial cells: Dependence upon AP-1 but not Ets. Mol Immunol. 2007 Feb;44(5):703-12.
19. Wake H, Moorhouse AJ, Jinno S, Kohsaka S, Nabekura J. Resting microglia directly monitor the functional state of synapses in vivo and determine the fate of ischemic terminals. J Neurosci. 2009 Apr 1;29(13):3974-80.
20. Hung J, Chansard M, Ousman SS, Nguyen MD, Colicos MA. Activation of microglia by neuronal activity: results from a new in vitro paradigm based on neuronal-silicon interfacing technology. Brain Behav Immun. 2010 Jan;24(1):31-40.
21. Jakubs K, Bonde S, Iosif RE, Ekdahl CT, Kokaia Z, Kokaia M, et al. Inflammation regulates functional integration of neurons born in adult brain. J Neurosci. 2008 Nov 19;28(47):12477-88.
22. Zhong Y, Zhou LJ, Ren WJ, Xin WJ, Li YY, Zhang T, et al. The direction of synaptic plasticity mediated by C-fibers in spinal dorsal horn is decided by Src-family kinases in microglia: the role of tumor necrosis factor-alpha. Brain Behav Immun. 2010 Aug;24(6):874-80.

23. Checchin D, Sennlaub F, Levavasseur E, Leduc M, Chemtob S. Potential role of microglia in retinal blood vessel formation. Invest Ophthalmol Vis Sci. 2006 Aug;47(8):3595-602.

24. Antony JM, Paquin A, Nutt SL, Kaplan DR, Miller FD. Endogenous microglia regulate development of embryonic cortical precursor cells. J Neurosci Res. 2011 Mar;89(3):286-98.

25. Chen SK, Tvrdik P, Peden E, Cho S, Wu S, Spangrude G, et al. Hematopoietic origin of pathological grooming in Hoxb8 mutant mice. Cell. 2010 May 28;141(5):775-85.

26. Rezaie P, Dean A, Male D, Ulfig N. Microglia in the cerebral wall of the human telencephalon at second trimester. Cereb Cortex. 2005 Jul;15(7):938-49.

27. Monier A, Adle-Biassette H, Delezoide AL, Evrard P, Gressens P, Verney C. Entry and distribution of microglial cells in human embryonic and fetal cerebral cortex. J Neuropathol Exp Neurol. 2007 May;66(5):372-82.

28. Cuadros MA, Navascues J. The origin and differentiation of microglial cells during development. Prog Neurobiol. 1998 Oct;56(2):173-89.

29. Rigato C, Buckinx R, Le-Corronc H, Rigo JM, Legendre P. Pattern of invasion of the embryonic mouse spinal cord by microglial cells at the time of the onset of functional neuronal networks. Glia. 2011 Apr;59(4):675-95.

30. Navascues J, Calvente R, Marin-Teva JL, Cuadros MA. Entry, dispersion and differentiation of microglia in the developing central nervous system. An Acad Bras Cienc. 2000;72(1):91-102.

31. Marin-Teva JL, Almendros A, Calvente R, Cuadros MA, Navascues J. Proliferation of actively migrating ameboid microglia in the developing quail retina. Anat Embryol (Berl). 1999 Sep;200(3):289-300.

32. Dalmau I, Vela JM, Gonzalez B, Finsen B, Castellano B. Dynamics of microglia in the developing rat brain. J Comp Neurol. 2003 Mar 31;458(2):144-57.

33. Navascues J, Moujahid A, Almendros A, Marin-Teva JL, Cuadros MA. Origin of microglia in the quail retina: central-to-peripheral and vitreal-to-scleral migration of microglial precursors during development. J Comp Neurol. 1995 Apr 3;354(2):209-28.

34. Cuadros MA, Moujahid A, Quesada A, Navascues J. Development of microglia in the quail optic tectum. J Comp Neurol. 1994 Oct 8;348(2):207-24.

35. Cuadros MA, Rodriguez-Ruiz J, Calvente R, Almendros A, Marin-Teva JL, Navascues J. Microglia development in the quail cerebellum. J Comp Neurol. 1997 Dec 22;389(3):390-401.

36. Marin-Teva JL, Almendros A, Calvente R, Cuadros MA, Navascues J. Tangential migration of ameboid microglia in the developing quail retina: mechanism of migration and migratory behavior. Glia. 1998 Jan;22(1):31-52.

37. Sanchez-Lopez A, Cuadros MA, Calvente R, Tassi M, Marin-Teva JL, Navascues J. Radial migration of developing microglial cells in quail retina: a confocal microscopy study. Glia. 2004 May;46(3):261-73.

38. Halfter W, Fua CS. Immunohistochemical localization of laminin, neural cell adhesion molecule, collagen type IV and T-61 antigen in the embryonic retina of the Japanese quail by in vivo injection of antibodies. Cell Tissue Res. 1987 Sep;249(3):487-96.

39. Liesi P, Silver J. Is astrocyte laminin involved in axon guidance in the mammalian CNS? Dev Biol. 1988 Dec;130(2):774-85.

40. Liesi P. Do neurons in the vertebrate CNS migrate on laminin? EMBO J. 1985 May;4(5):1163-70.

41. Stewart GR, Pearlman AL. Fibronectin-like immunoreactivity in the developing cerebral cortex. J Neurosci. 1987 Oct;7(10):3325-33.

42. Sheppard AM, Hamilton SK, Pearlman AL. Changes in the distribution of extracellular matrix components accompany early morphogenetic events of mammalian cortical development. J Neurosci. 1991 Dec;11(12):3928-42.

43. Tanzer ML. Current concepts of extracellular matrix. J Orthop Sci. 2006 May;11(3):326-31.

44. Milner R, Campbell IL. Cytokines regulate microglial adhesion to laminin and astrocyte extracellular matrix via protein kinase C-dependent activation of the alpha6beta1 integrin. J Neurosci. 2002 Mar 1;22(5):1562-72.

45. Milner R, Campbell IL. The extracellular matrix and cytokines regulate microglial integrin expression and activation. J Immunol. 2003 Apr 1;170(7):3850-8.

46. Jung S, Aliberti J, Graemmel P, Sunshine MJ, Kreutzberg GW, Sher A, et al. Analysis of fractalkine receptor CX(3)CR1 function by targeted deletion and green fluorescent protein reporter gene insertion. Mol Cell Biol. 2000 Jun;20(11):4106-14.

47. Chan WY, Kohsaka S, Rezaie P. The origin and cell lineage of microglia: new concepts. Brain Res Rev. 2007 Feb;53(2):344-54.

48. Patterson PH, Xu W, Smith S.E.P, Devarman B.E. Maternal Imunne Activation, Cytokines and Autism. AW Zimmerman (ed), Autism. 2008.

49. Rezaie P, Male D. Colonisation of the developing human brain and spinal cord by microglia: a review. Microsc Res Tech. 1999 Jun 15;45(6):359-82.

50. Rezaie P, Trillo-Pazos G, Greenwood J, Everall IP, Male DK. Motility and ramification of human fetal microglia in culture: an investigation using time-lapse video microscopy and image analysis. Exp Cell Res. 2002 Mar 10;274(1):68-82.

51. Stence N, Waite M, Dailey ME. Dynamics of microglial activation: a confocal time-lapse analysis in hippocampal slices. Glia. 2001 Mar 1;33(3):256-66.

52. Grossmann R, Stence N, Carr J, Fuller L, Waite M, Dailey ME. Juxtavascular microglia migrate along brain microvessels following activation during early postnatal development. Glia. 2002 Mar 1;37(3):229-40.

53. Carbonell WS, Murase S, Horwitz AF, Mandell JW. Migration of perilesional microglia after focal brain injury and modulation by CC chemokine receptor 5: an in situ time-lapse confocal imaging study. J Neurosci. 2005 Jul 27;25(30):7040-7.

54. Sheppard AM, Brunstrom JE, Thornton TN, Gerfen RW, Broekelmann TJ, McDonald JA, et al. Neuronal production of fibronectin in the cerebral cortex during migration and layer formation is unique to specific cortical domains. Dev Biol. 1995 Dec;172(2):504-18.

55. Nadarajah B, Brunstrom JE, Grutzendler J, Wong RO, Pearlman AL. Two modes of radial migration in early development of the cerebral cortex. Nat Neurosci. 2001 Feb;4(2):143-50.

56. Lee JE, Liang KJ, Fariss RN, Wong WT. Ex vivo dynamic imaging of retinal microglia using time-lapse confocal microscopy. Invest Ophthalmol Vis Sci. 2008 Sep;49(9):4169-76.

57. Milner R, Campbell IL. The integrin family of cell adhesion molecules has multiple functions within the CNS. J Neurosci Res. 2002 Aug 1;69(3):286-91.

58. Whitley M, Treloar H, De Arcangelis A, Georges Labouesse E, Greer CA. The alpha6 integrin subunit in the developing mouse olfactory bulb. J Neurocytol. 2005 Mar;34(1-2):81-96.

59. Romberger DJ. Fibronectin. Int J Biochem Cell Biol. 1997 Jul;29(7):939-43.

60. Chun JJ, Shatz CJ. A fibronectin-like molecule is present in the developing cat cerebral cortex and is correlated with subplate neurons. J Cell Biol. 1988 Mar;106(3):857-72.

61. Stettler EM, Galileo DS. Radial glia produce and align the ligand fibronectin during neuronal migration in the developing chick brain. J Comp Neurol. 2004 Jan 12;468(3):441-51.

62. Tarone G, Hirsch E, Brancaccio M, De Acetis M, Barberis L, Balzac F, et al. Integrin function and regulation in development. Int J Dev Biol. 2000;44(6):725-31.

63. Yoshida N, Hishiyama S, Yamaguchi M, Hashiguchi M, Miyamoto Y, Kaminogawa S, et al. Decrease in expression of alpha 5 beta 1 integrin during neuronal differentiation of cortical progenitor cells. Exp Cell Res. 2003 Jul 15;287(2):262-71.

64. Marchetti G, Escuin S, van der Flier A, De Arcangelis A, Hynes RO, Georges-Labouesse E. Integrin alpha5beta1 is necessary for regulation of radial migration of cortical neurons during mouse brain development. Eur J Neurosci. 2010 Feb;31(3):399-409.

65. Chamak B, Mallat M. Fibronectin and laminin regulate the in vitro differentiation of microglial cells. Neuroscience. 1991;45(3):513-27.

SUPPLEMENTAL INFORMATION

1 Introduction supplement

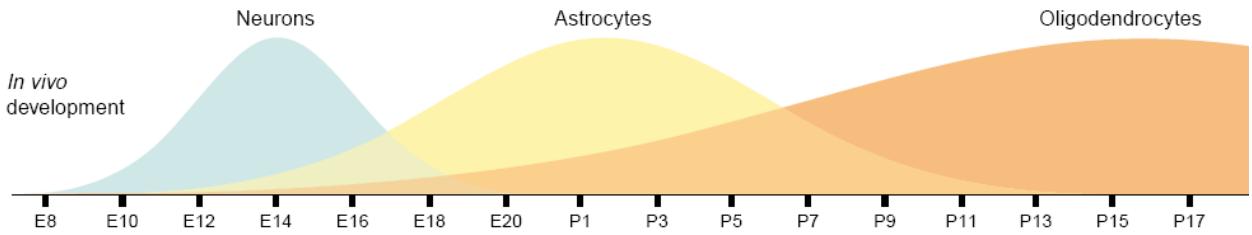

Supplemental figure 1. *In vivo* development of cortical neurons and macroglia in rats. E, Embryonic day; P, Postnatal day. *Adapted from Sauvageot CM, Stiles CD. Curr Opin Neurobiol 2002, 12(3):244-9*

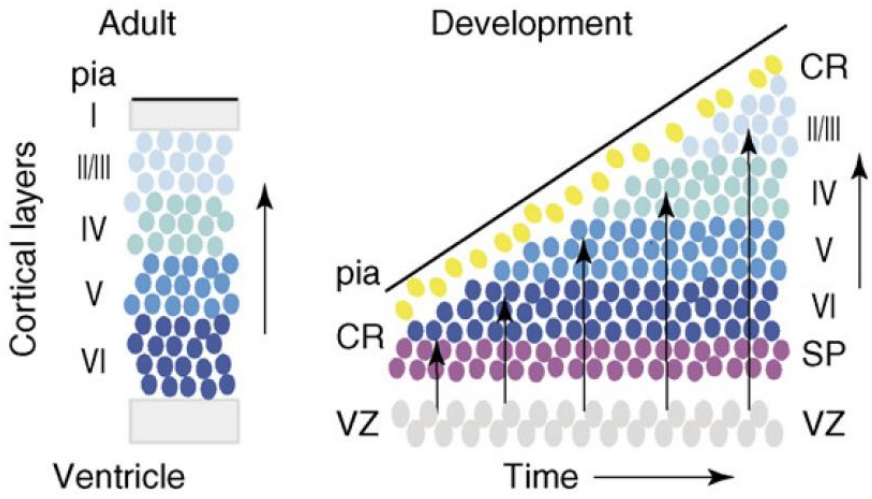

Supplemental figure 2. Neocortex development. First born neurons migrate to the deepest cortical layers (dark blue). Subsequently produced neurons migrate to more successively superficial layers (lighter blues) creating an inside-out order lamination. VZ, ventricular zone; SP, subplate; CR, Cajal-Retzius cells. *Adapted from Cooper JA. Trends Neurosci 2008, 31(3):113-9*

2 Material & methods supplement

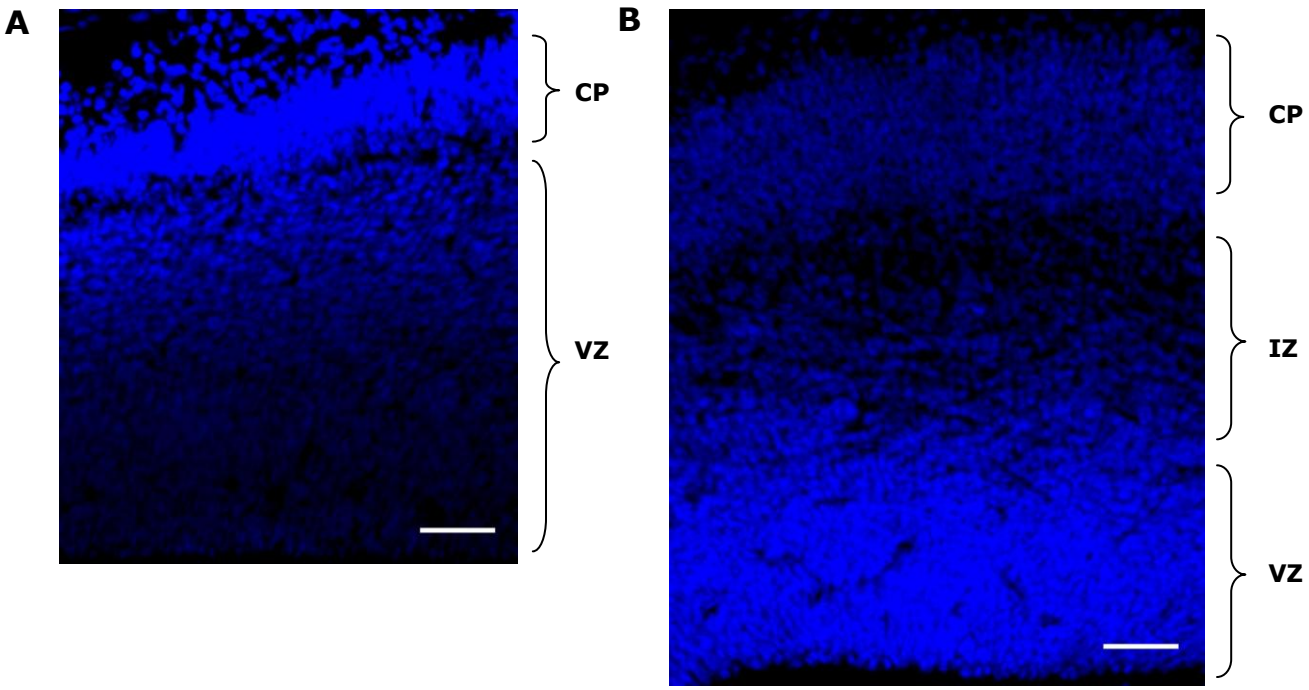

Supplemental figure 3. Classification of the morphological zones in E14.5 (A) and E15.5 (B). DAPI nuclear staining (blue). VZ, ventricular zone; CP, cortical plate; IZ, intermediate zone. Scale bar= 50µm

3 Results supplement

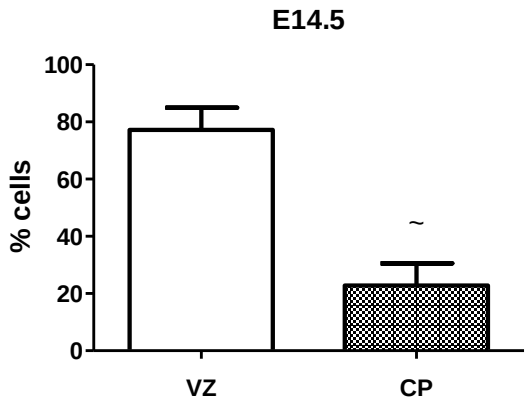

Supplemental figure 4. Location of microglia at E14.5 in different cortical zones. At E14.5, microglia tend to be situated more in the ventricular zone (VZ), than in the cortical plate (CP) (N=3). Means ± SEM are indicated. Mann Whitney test was performed with ~=p<0.1.

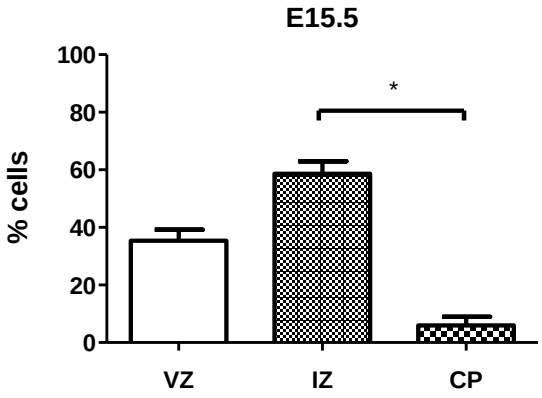

Supplemental figure 5. Location of microglia at E15.5 in different cortical zones. At E15.5, microglia are situated more in intermediate zone (IZ), than in the cortical plate (CP) (N=3). Means ± SEM are indicated. Kruskal-Wallis test followed by Dunn's Multiple Comparison test were applied. *=p<0.05. VZ, ventricular zone.

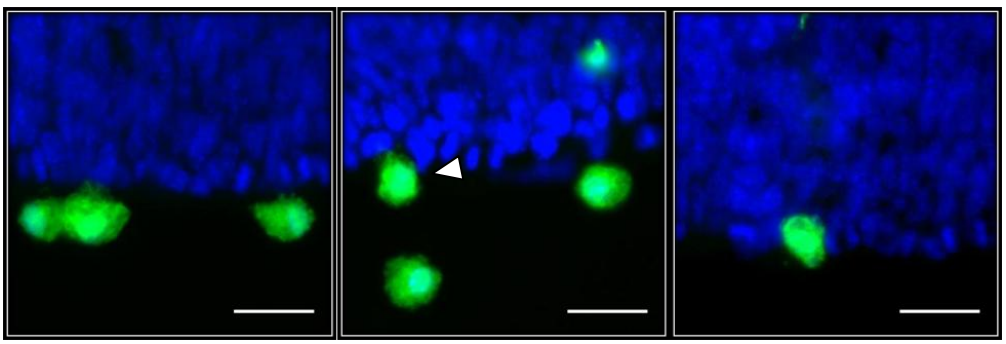

Supplemental figure 6. Amoeboid microglia entering the neocortical parenchyma. E15.5 coronal mouse brain sections. Microglia expressing eGFP (green) and DAPI nuclear staining (blue) in the neocortex. **A.** Microglia sending out short protrusions contacting the cells lining the ventricular lumen. **B.** Microglial cell penetrating the ventricular lining (arrowhead). **C.** Microglial cell which has just entered the neocortex and is continuing its journey. Scale bar=20µm.

Supplemental table 1. Sum of absolute migrated distances (µm) between successive time points in X,Y and Z coordinates. Numbers in bold indicate the highest sum for X or Y. Cells that were not in the field of view during the full 7 hours were excluded from the analysis.

Cell Nr.	2010v1126(E14.5)			2010v1047(E14.5)			2010v1124(E14.5)			2010v26(E15.5)		
	X	**Y**	**Z**	**X**	**Y**	**Z**	**X**	**Y**	**Z**	**X**	**Y**	**Z**
1	240	**321,9**	32	112,7	**139,3**	16	115,9	**146,7**	0	203,6	**148,4**	32
2	109,4	**159,5**	56	**132,7**	124,7	32	/	/	/	**91,6**	109,7	32
3	97,5	**249,4**	32	**197,2**	175,1	32	**142,9**	107,1	64	**104**	110,6	72
4	**186,9**	186,3	8	**214,8**	179	72	**179,4**	178,5	48	79,1	**56,9**	24
5	112,3	**295,2**	8	74,8	**149,7**	48	109,2	**207,8**	64	/	/	/
6	77	**125,7**	8	142,6	**173,2**	56	142,7	**147**	16	**91,4**	109,9	24
7	54,4	**57**	0	**202,8**	188,7	64	167,7	**178,5**	56	**70**	110	56
8	59,8	**91,6**	0	**89,2**	71	16	113,9	**124,1**	16	**68,6**	101,6	16
9	102,8	**115,9**	48	94	**154,1**	48	102,5	**122**	64	129	**116,9**	48
10	124,9	**170,2**	24	127,3	**163,1**	0	76,1	**113,6**	16	160,8	**132,8**	64
11	/	/	/	78,1	**82,6**	40	**122,8**	114,8	24	241,4	**121,3**	56
12	49,3	**88,9**	16				129,1	**140,5**	24	165,3	**138,8**	24
13	71,9	**118,4**	24				**99,3**	62,6	16	222,5	**149,1**	48
14	110,9	**197,5**	24				99,5	**104,8**	32	126,6	**116**	40
15							90,7	**111,5**	32	202,4	**120,4**	40
16							**81,9**	78,1	24	**175**	73,7	24

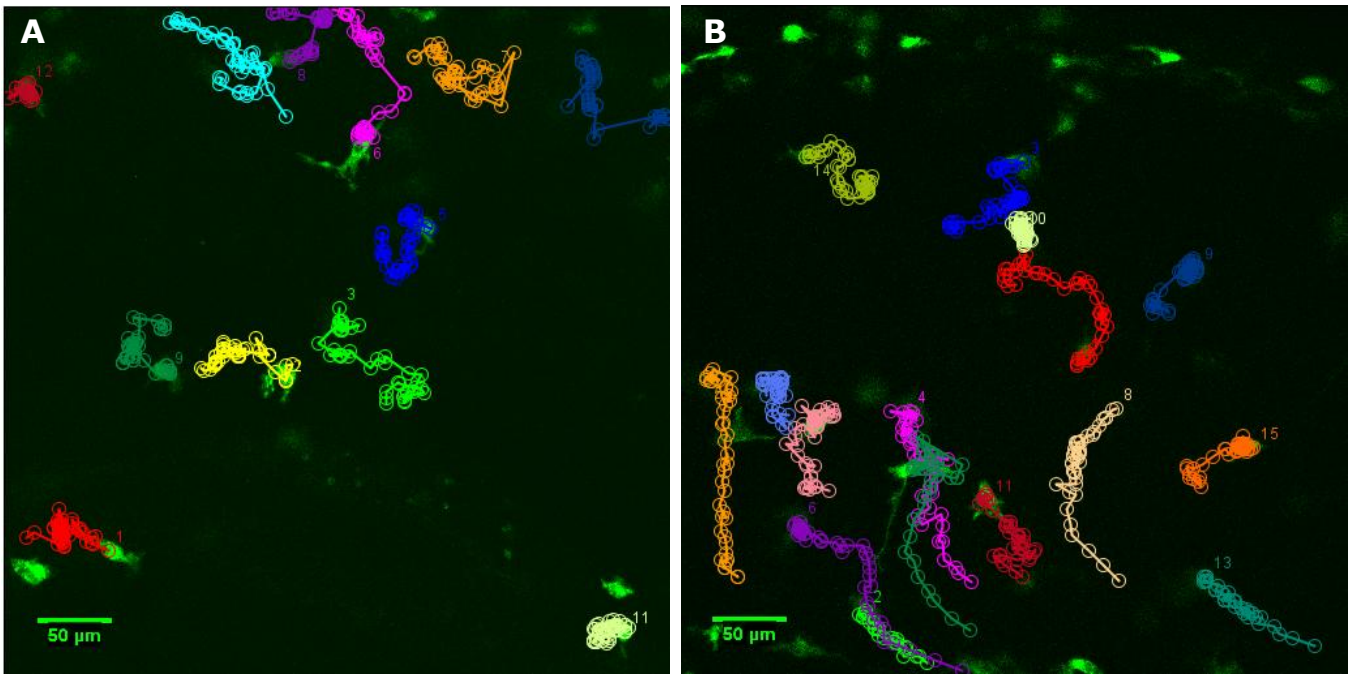

Supplemental figure 7. Microglial migration pathways in the E14.5 neocortex of 2 other experiments. Colored connected circles represent the location of the microglial soma at each time point. Track numbers indicate the last time point. The pia is located on top, marked by the high density of bright fluorescent microglia.

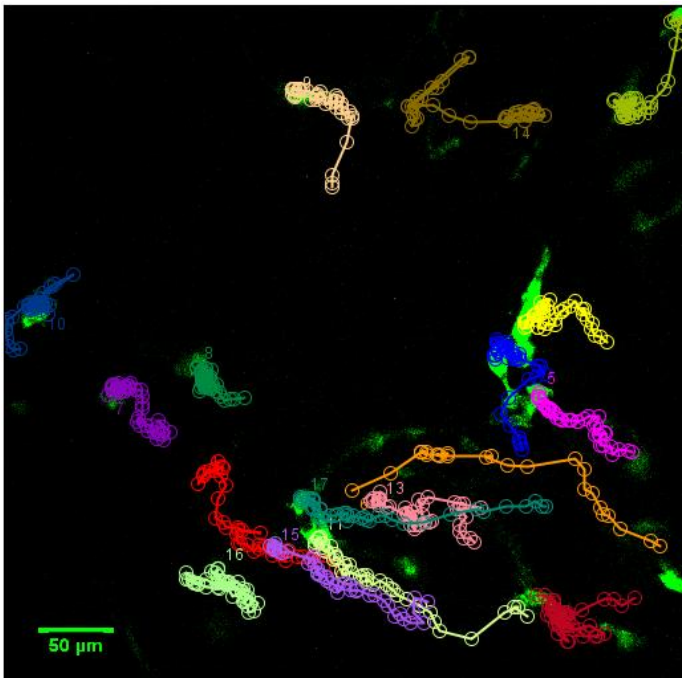

Supplemental figure 8. Microglial migration pathways in the E15.5 neocortex. Colored connected points represent the location of the microglial soma at each time point. Track numbers indicate the last time point. The pia is located on top, but outside the field of view.

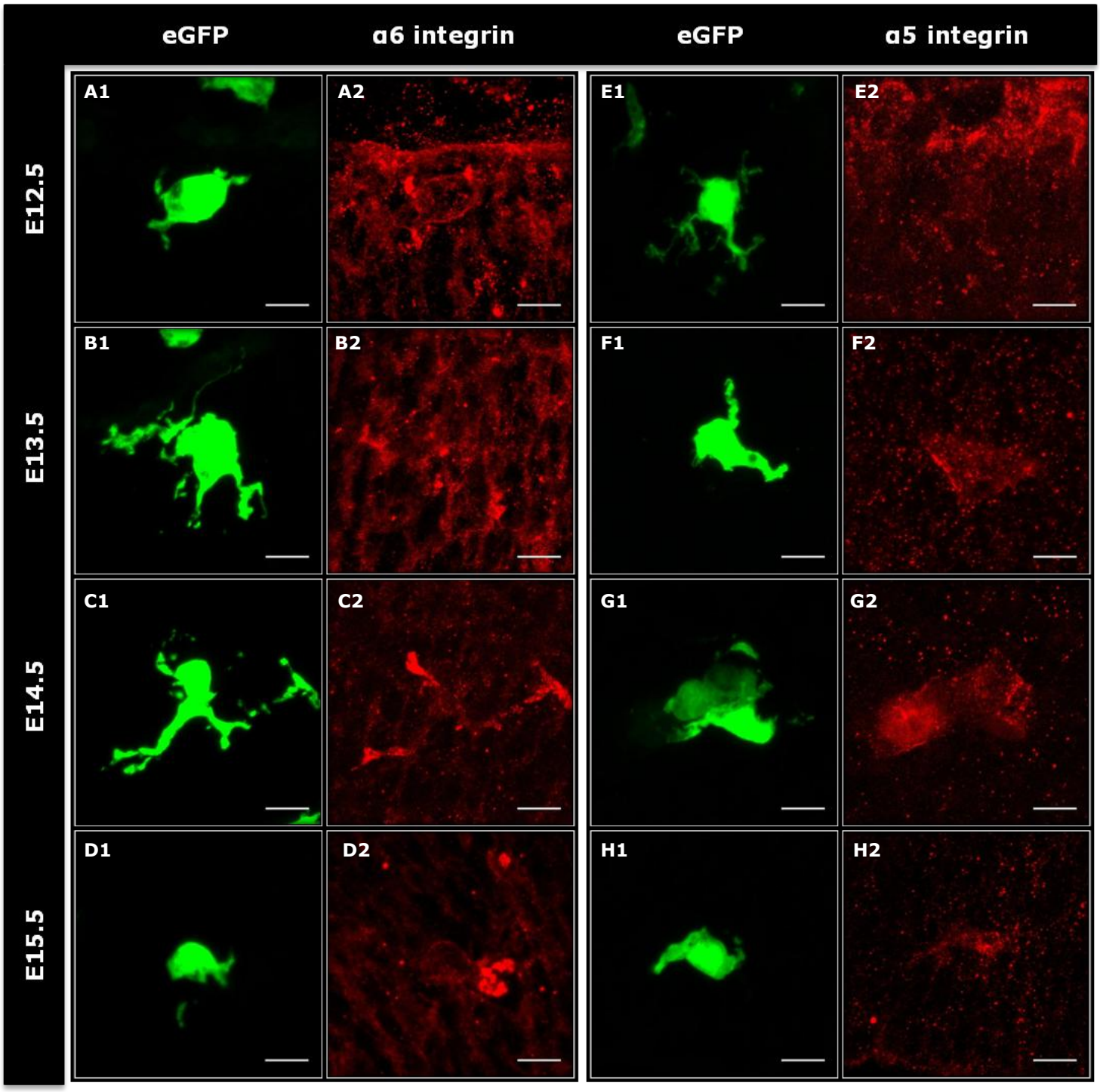

Supplemental figure 9. LMR and FNR expression by microglia in the embryonic neocortex. Images are Z-projections and correspond to the Zoom+merge parts from Fig. 18 and 20. Microglia expressing eGFP (green) from E12.5-E15.5 are shown in A1-D1 and E1-H1. **A-D.** Staining against α6 integrin (A555-red), to visualize the LMR. Microglial imprints can be clearly distinguished. **E-H.** Staining against α5 integrin (A555-red), to visualize the FNR. Microglia are characterized by a very weak expression of the FNR. Scale bar=10μm.

Auteursrechtelijke overeenkomst

Ik/wij verlenen het wereldwijde auteursrecht voor de ingediende eindverhandeling:
Migration of microglia in the embryonic neocortex

Richting: **master in de biomedische wetenschappen-klinische moleculaire wetenschappen**
Jaar: **2011**

in alle mogelijke mediaformaten, - bestaande en in de toekomst te ontwikkelen - , aan de Universiteit Hasselt.

Niet tegenstaand deze toekenning van het auteursrecht aan de Universiteit Hasselt behoud ik als auteur het recht om de eindverhandeling, - in zijn geheel of gedeeltelijk -, vrij te reproduceren, (her)publiceren of distribueren zonder de toelating te moeten verkrijgen van de Universiteit Hasselt.

Ik bevestig dat de eindverhandeling mijn origineel werk is, en dat ik het recht heb om de rechten te verlenen die in deze overeenkomst worden beschreven. Ik verklaar tevens dat de eindverhandeling, naar mijn weten, het auteursrecht van anderen niet overtreedt.

Ik verklaar tevens dat ik voor het materiaal in de eindverhandeling dat beschermd wordt door het auteursrecht, de nodige toelatingen heb verkregen zodat ik deze ook aan de Universiteit Hasselt kan overdragen en dat dit duidelijk in de tekst en inhoud van de eindverhandeling werd genotificeerd.

Universiteit Hasselt zal mij als auteur(s) van de eindverhandeling identificeren en zal geen wijzigingen aanbrengen aan de eindverhandeling, uitgezonderd deze toegelaten door deze overeenkomst.

Voor akkoord,

Smolders, Sophie

Datum: **14/06/2011**